Obrysová analýza: Analýza vlastných tvarov - Eigenshape analysis

Radius function – polomerová funkcia r(θ)

Referenčná línia je polomer vedený od centroidu (alebo iného bodu v zodpovedajúcej polohe) k základnému význačnému bodu. Od tohto polomeru sa v rovnakých uhloch vedú ďalšie línie. Polomerová funkcia opisuje vzťah medzi uhlom rotácie a zodpovedajúcou dĺžkou polomeru.

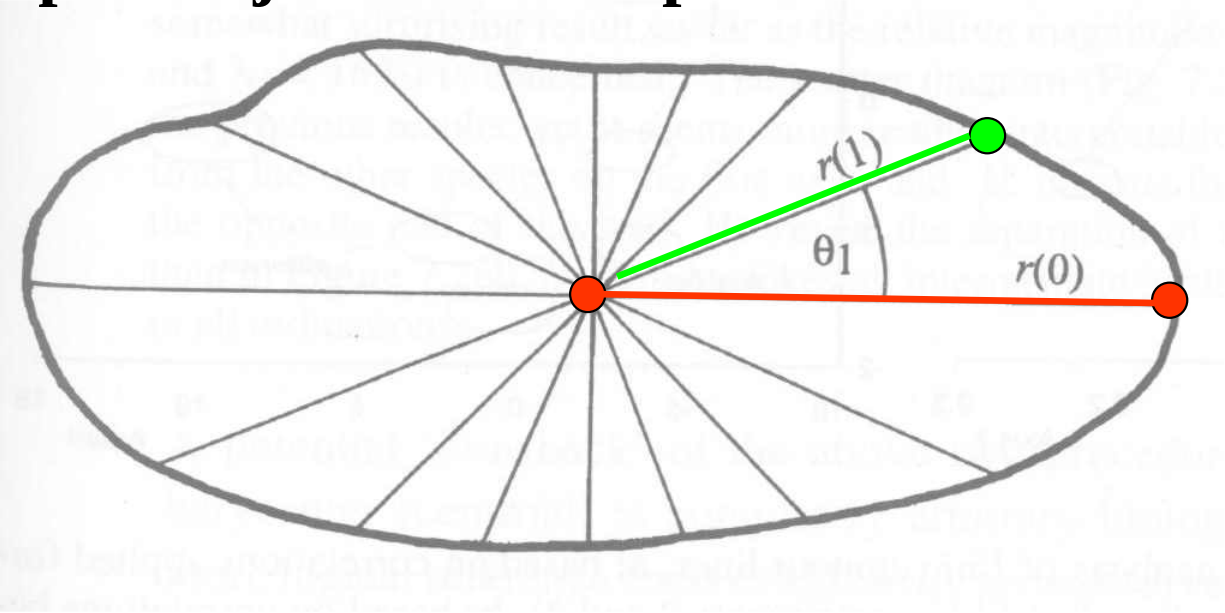

Podani (2000)

Analýza vlastných tvarov - Eigenshape analysis

Radius function – polomerová funkcia r(θ)

Pokiaľ je počet polomerov vedených od centroidu dostatočný počet (*p*) ich dĺžky pomerne dobre popisujú sledovaný tvar.

Výsledkom je matica $p \times m$, kde *m* je počet sledovaných objektov. Matica je podkladom pre PCA, ktorá je založená na korelácii medzi objektmi (nie medzi znakmi) – analýza vlastných tvarov.

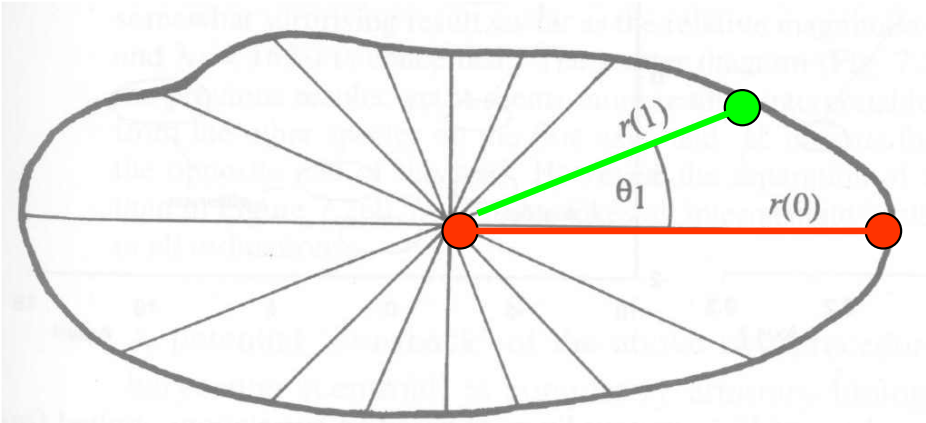

Podani (2000)

Analýza vlastných tvarov - Eigenshape analysis

Radius function – polomerová funkcia r(θ)

Unio PCA – eigenshape analysis, prvé vlastné číslo 97% - komponent veľkosti, preto je potom lepšie posudzovať druhú a tretiu os

Unio PCA – korelácie znakov, prvé vlastné číslo 91,3 %, druhé 5,2%

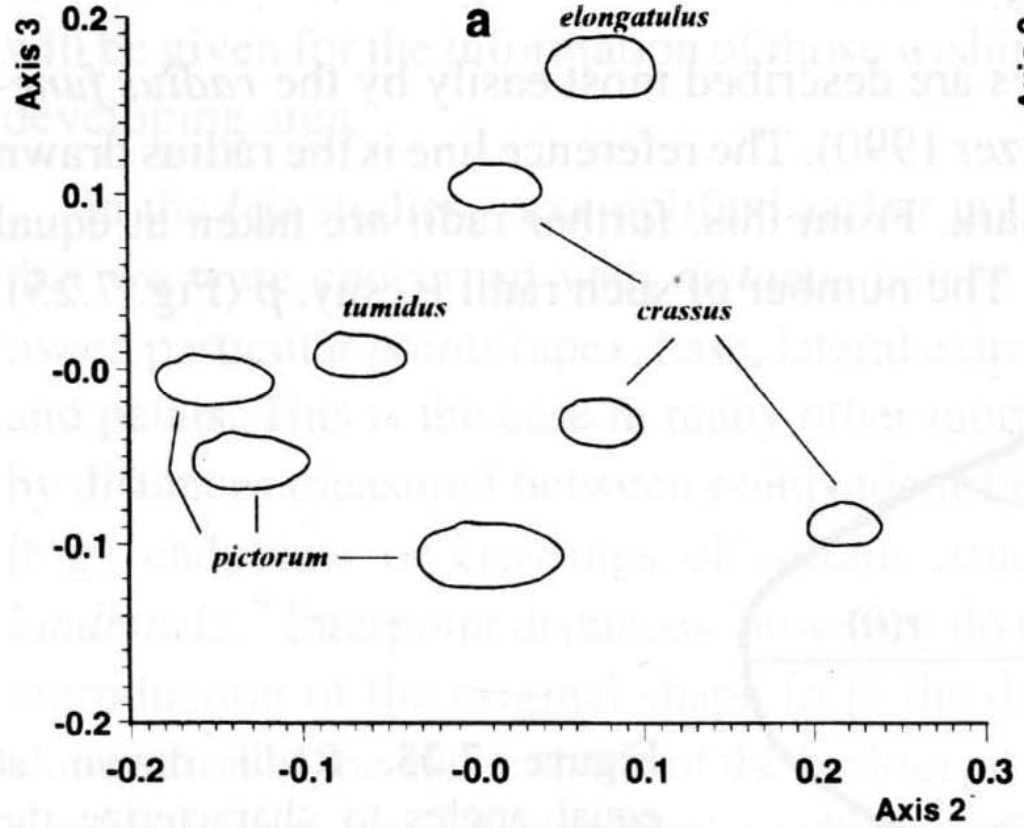

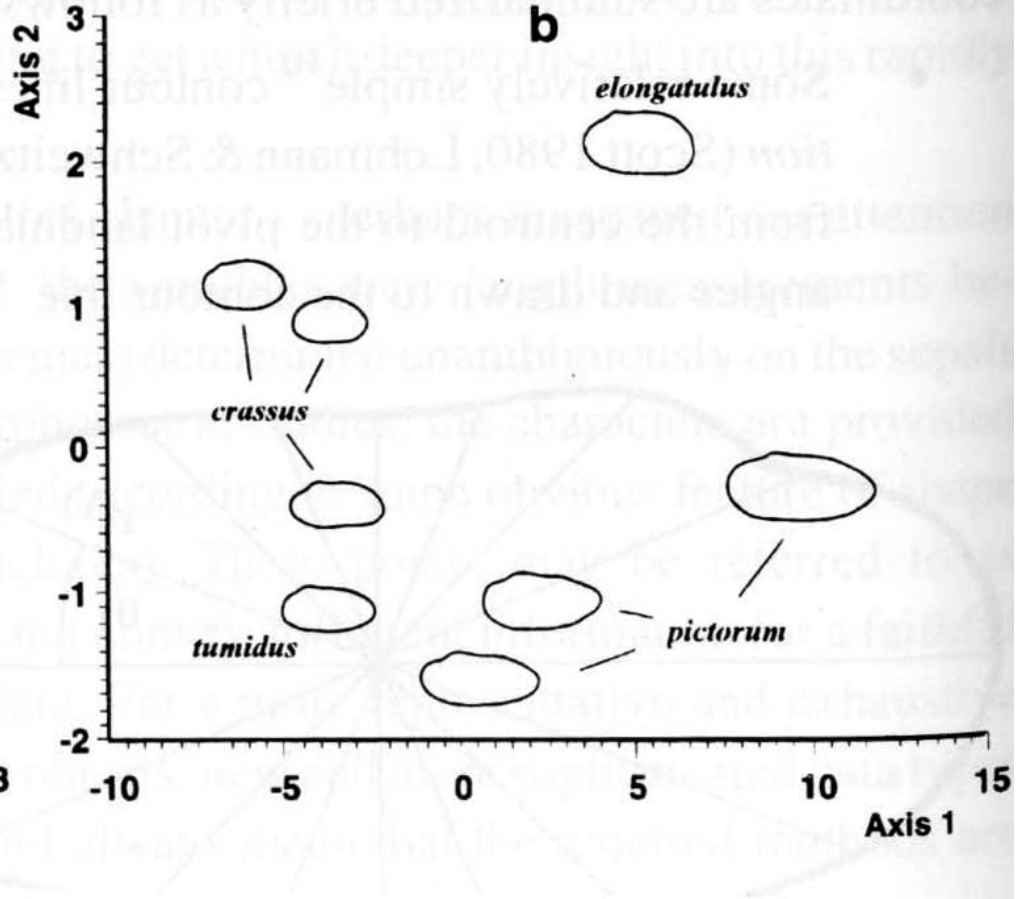

Podani (2000)

Analýza vlastných tvarov - Eigenshape analysis

Radius function – polomerová funkcia r(θ)

Pre zložitejšie tvary táto funkcia nie je vhodná pre opis zložitejších tvarov – v niektorých prípadoch r nemá jedinú hodnotu pre daný uhol θ.

Problematická je aj voľba centrálneho význačného bodu alebo centroidu – ak je jeho pozícia variabilná vo vzťahu k biol. štruktúre potom výrazne ovplyvňuje výsledok

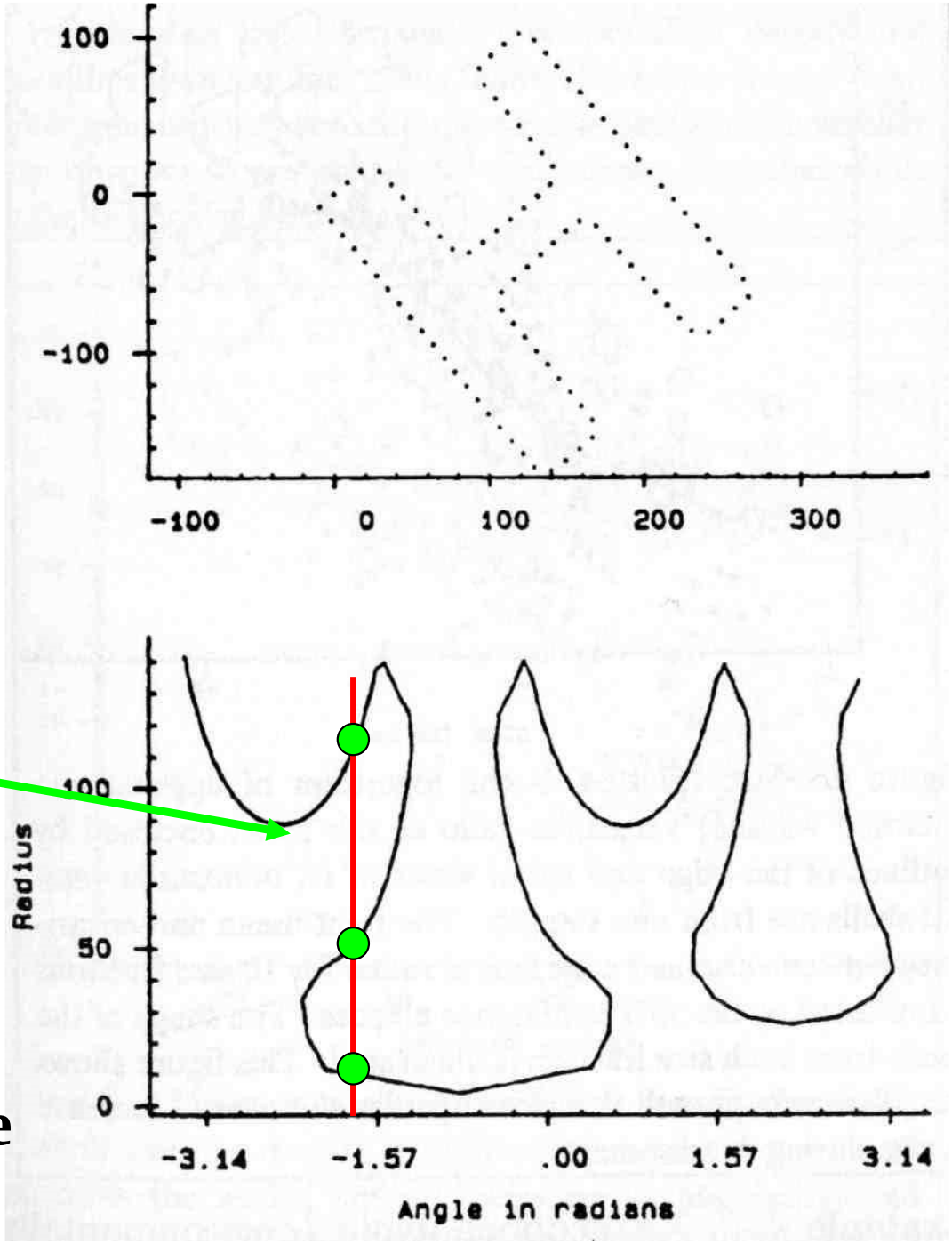

Lohmann & Schweitzer (1990, „Blue Book“)

Analýza vlastných tvarov - Eigenshape analysis

Zahnova a Roskiesova funkcia tvaru – Zahn & Roskies‘ shape function $\varphi^*(t) = \varphi(t) - t$

t je vzdialenosť od počiatočného (nulového) význačného bodu pozdĺž obrysu, ktorý je normalizovaný na celkovú dĺžku 2πr, φ (*t*) je uhol medzi tangenciálnym vektorom v bode 0 a vektorom vo vzdialenosti t od nulového bodu v radiánoch.

Funkcia má nulovú hodnotu pre kruhový obrys.

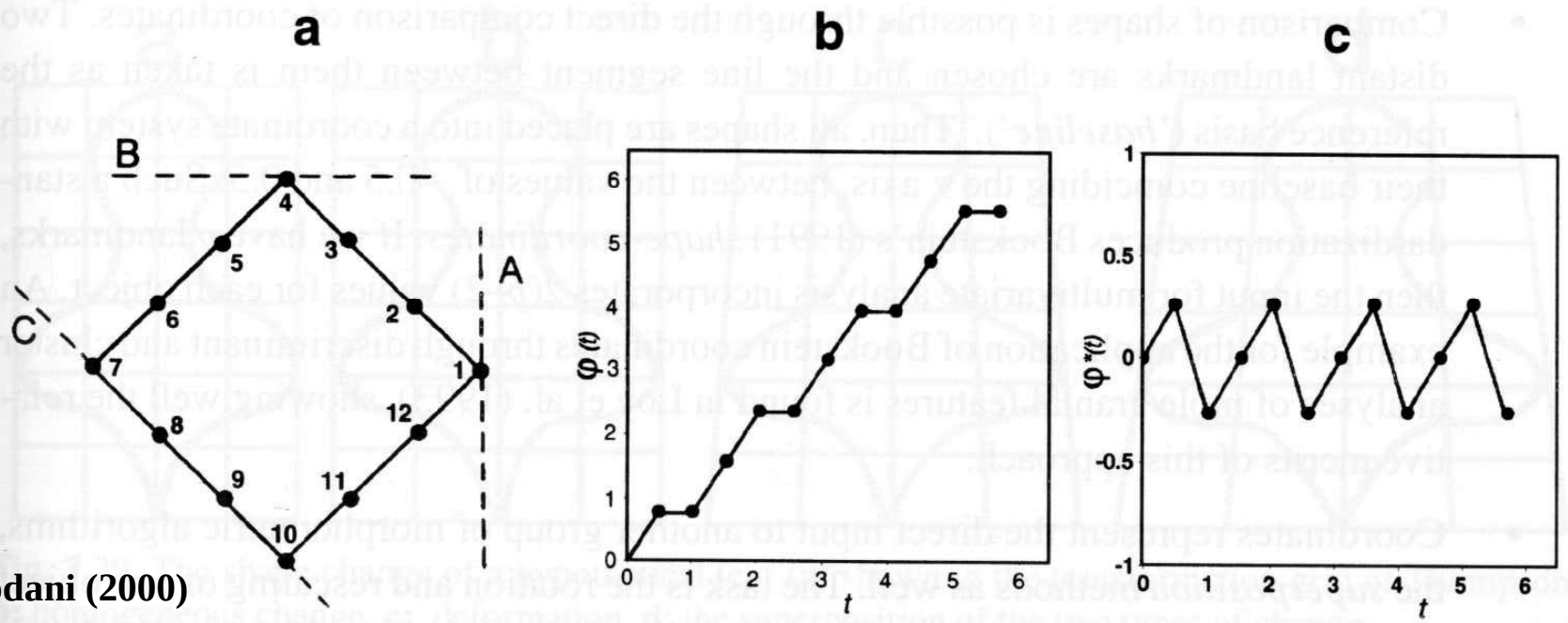

Podani (2000)

Analýza vlastných tvarov - Eigenshape analysis

Zahnova a Roskiesova funkcia tvaru – Zahn & Roskies‘ shape function

$$\varphi^*(t) = \varphi(t) - t$$

Výsledkom je matica, ktorá sa použije na analýzu vlastných tvarov (PCA). „Sampling“ obrysu teda nie je v rovnakých uhloch ale v rovnakých vzdialenostiach pozdĺž obrysu, čím sú tieto vzdialenosti kratšie, tým je výsledok presnejší (min. *n* = 100).

Tvar – funkcia $\varphi^*(t)$

Veľkosť – S = t / n

Angularita - amplitúda

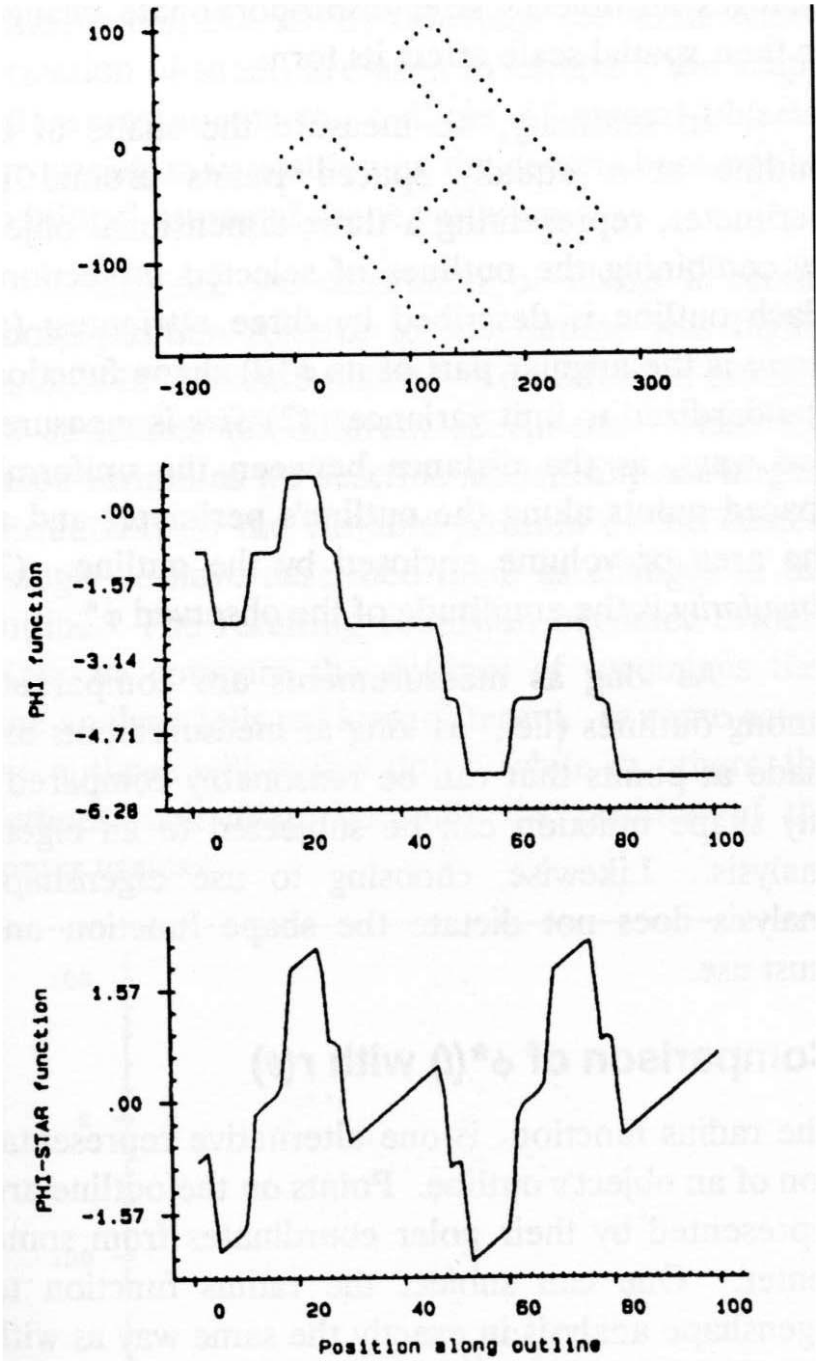

Lohmann & Schweitzer (1990, „Blue Book“)

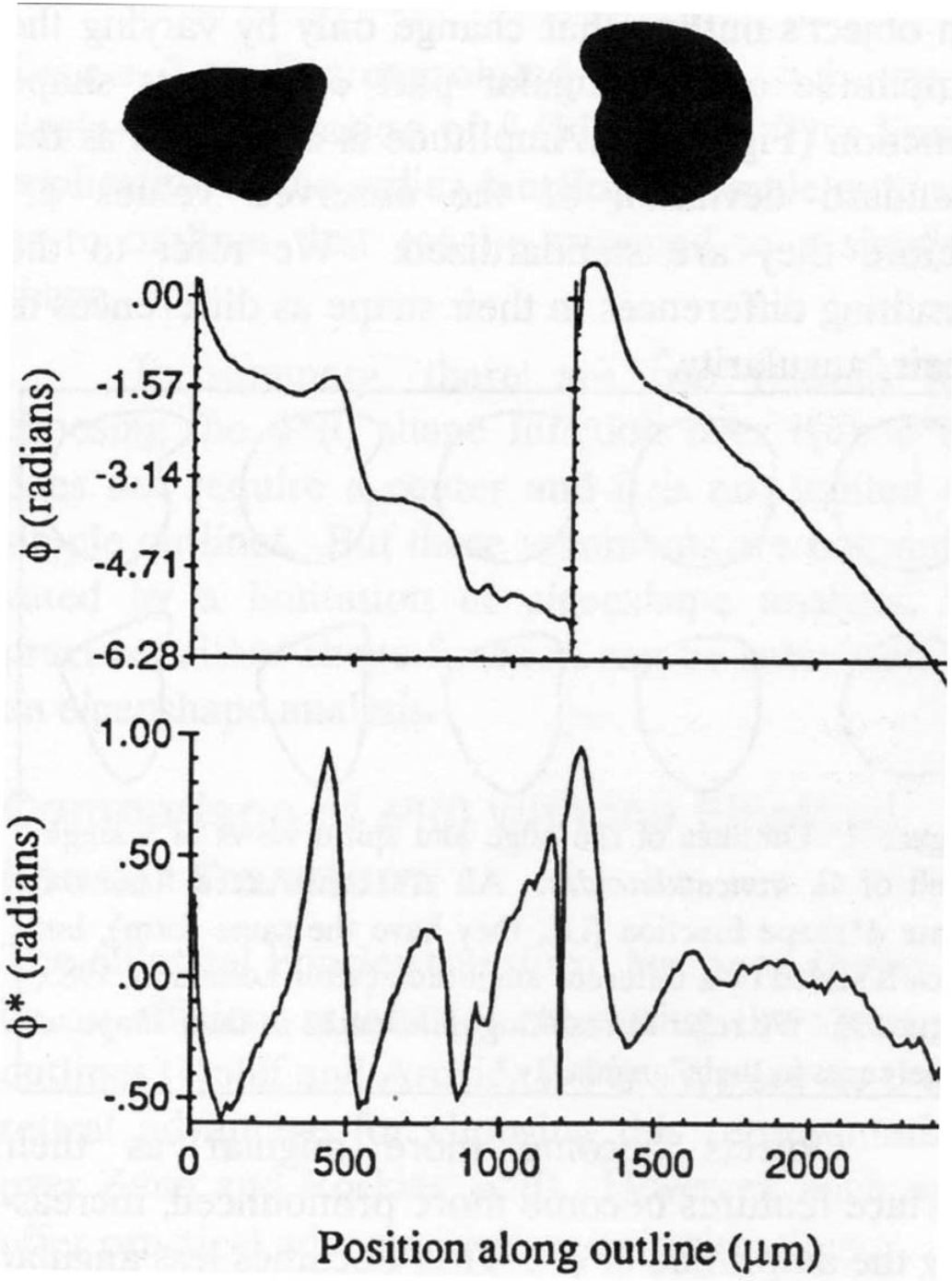

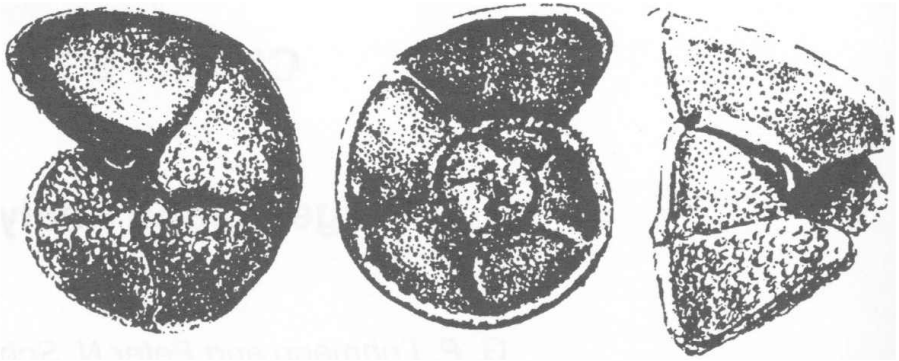

Globorotalia truncatulinoides

Dôležitý je počiatočný význačný bod a smer zberu dát pozdĺž obrysu ! (po smere alebo proti smeru hodinových ručičiek)

Lohmann & Schweitzer (1990, „Blue Book“)

Analýza vlastných tvarov - Eigenshape analysis

Zahnova a Roskiesova funkcia tvaru – Zahn & Roskies‘ shape function

funkcie tvaru

vlastné funkcie tvaru

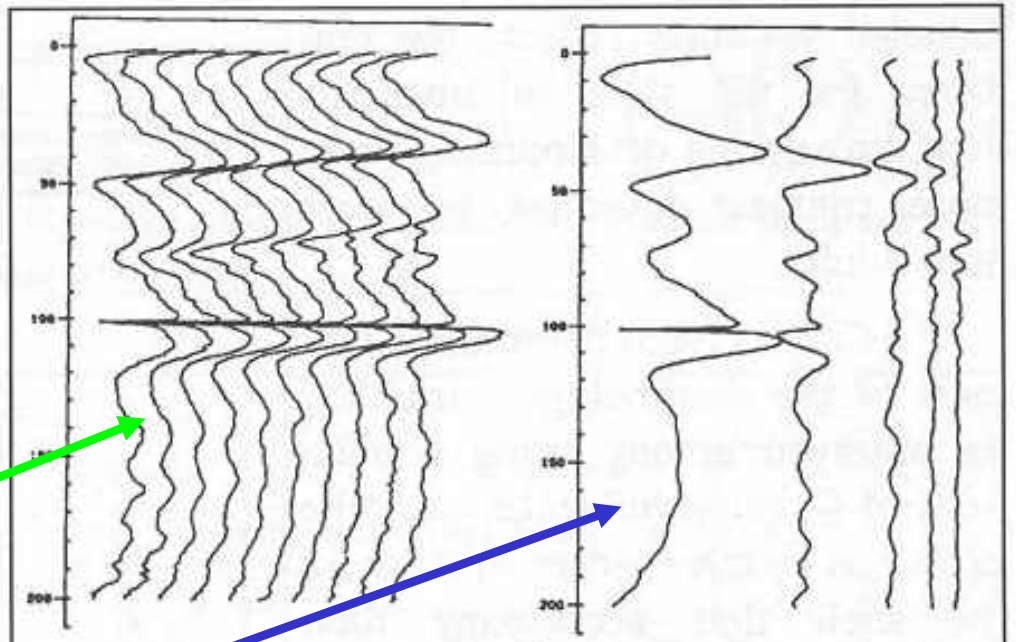

Figure 14. Zahn and Roskies' $\phi^*(\ell)$ shape functions (plotted on the left) of the combined edge and spiral views of *G. truncatulinoides* shown in Figure 13 and their first 5 eigenshape functions (plotted on the right). See Figure 11 for explanation.

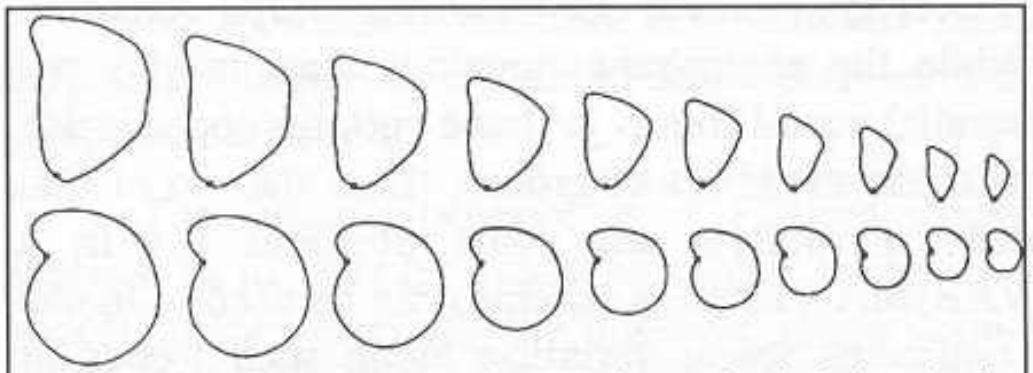

Figure 13. The average outlines (edge and spiral views) of the shells of *G. truncatulinoides* from 10 size-fractions of a single sample. The outlines are plotted to the same scale, the starting reference point is indicated, and the outline of each view is drawn between 100 equally spaced points.

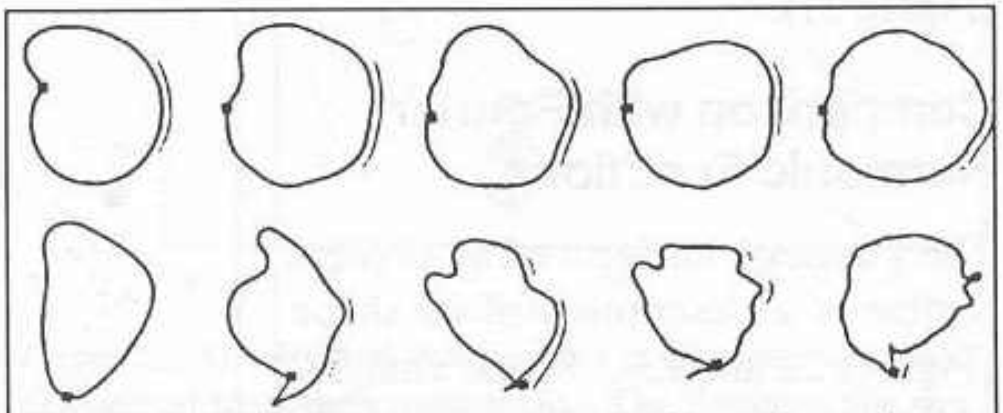

Figure 15. Shape outlines constructed from the 5 eigenshape functions plotted in Figure 14 (rebuilt and plotted by program CSHAPE). The implicit 90° turn between the combined outlines separates the edge and spiral views of the eigenshapes.

Lohmann & Schweitzer (1990, „Blue Book“)

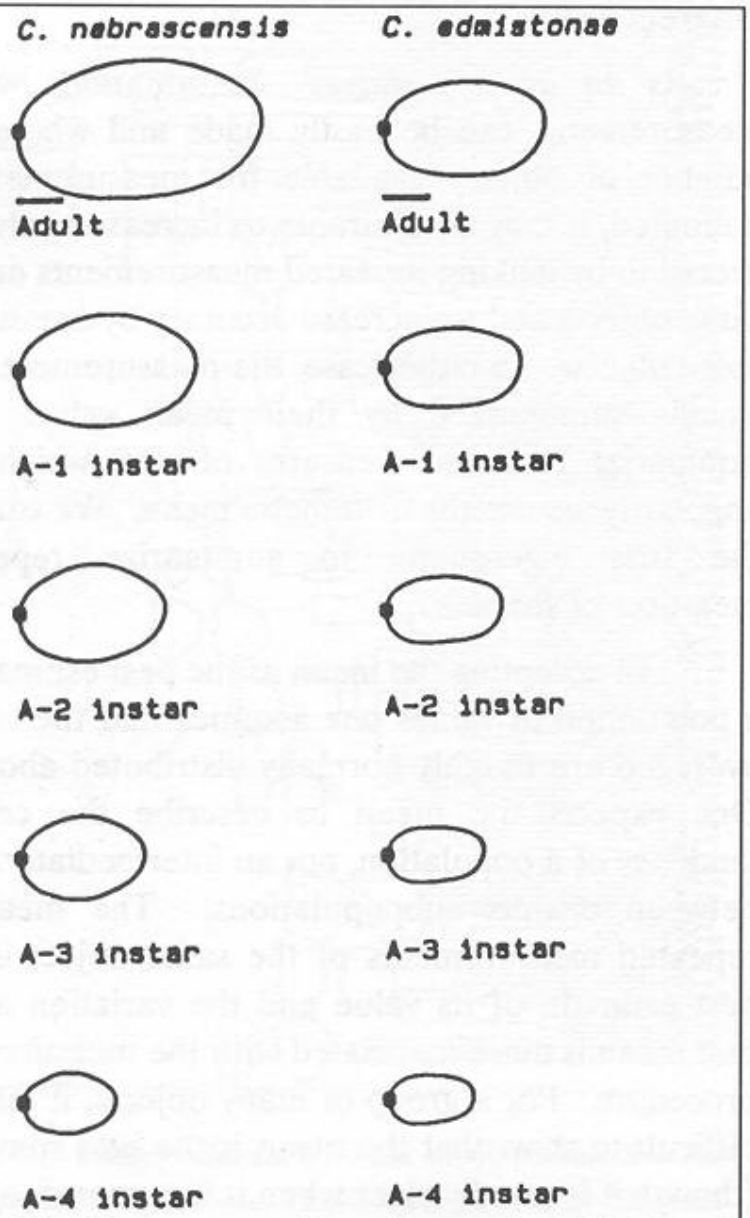

Figure 10. The average outlines of ostracode shells from 5 instars (growth stages) in each of two related species of *Cavellina* (from Schweitzer et al., 1986). The outlines are plotted to the same scale, the starting reference point is indicated, and each outline is drawn between 128 equally spaced points.

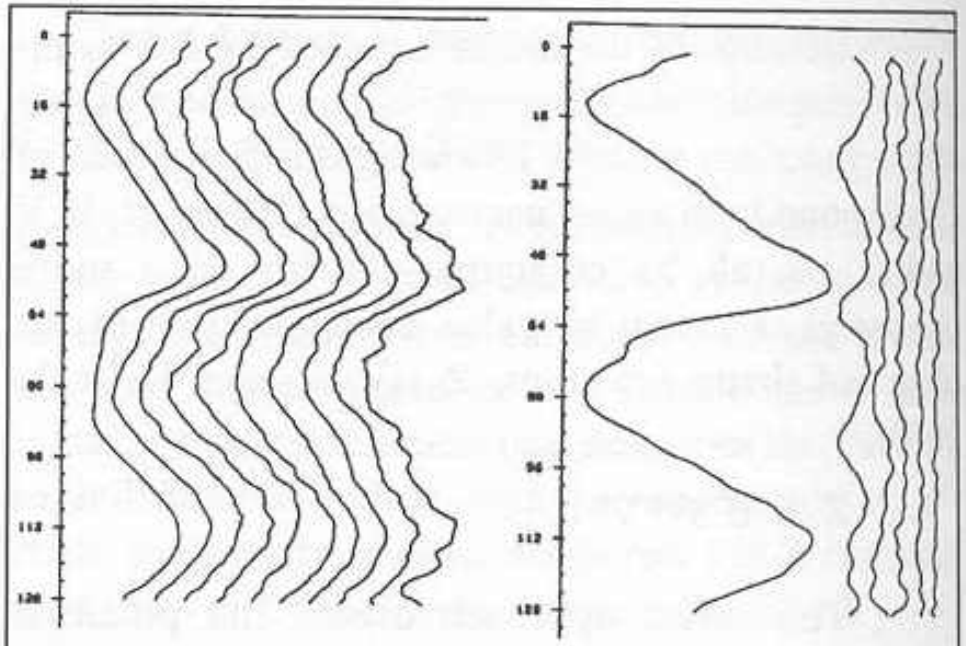

Figure 11. Zahn and Roskies' $\phi^*(\ell)$ shape functions (on the left) of the ostracode outlines shown in Figure 10 and their first 5 eigenshape functions (on the right). The values of ϕ^*, the net angular bend around each outline, are plotted on the horizontal axis. The vertical axis orders the 128 comparable points located around the perimeter of each outline.

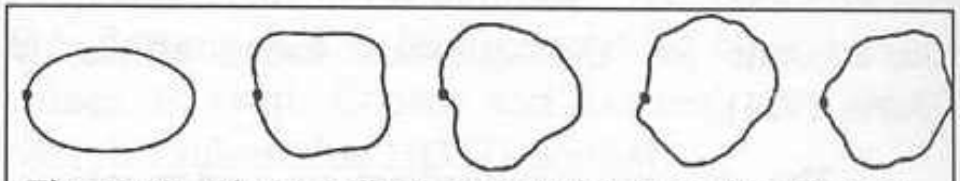

Figure 12. Shape oulines constructed from the 15 eigenshape functions plotted in Figure 11 (rebuilt and plotted by program CSHAPE). Only the first eigenshape resembles the ostracodes that were analyzed. Since it accounts for most of the "variance" among a collection of similar objects, it describes features they all share, features that make them look the same, and it approximates the mean shape. The other eigenshapes account for the remaining "variance" contributed by features that make the objects look different.

Lohmann & Schweitzer (1990, „Blue Book“)

Paleobiology, 27(2), 2001, pp. 226–240

The role of phylogeny in quantitative paleobiological data analysis

Norman MacLeod

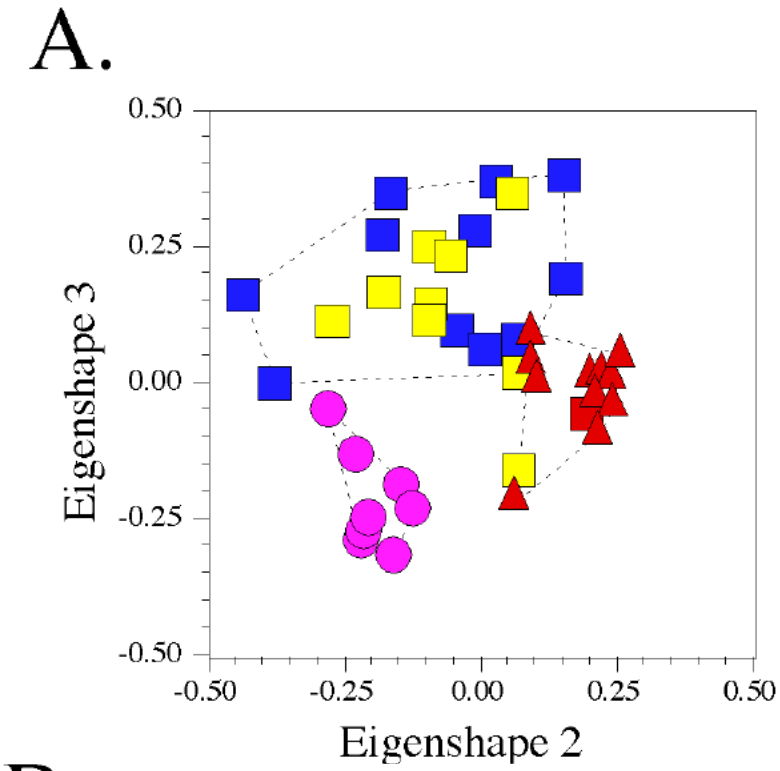

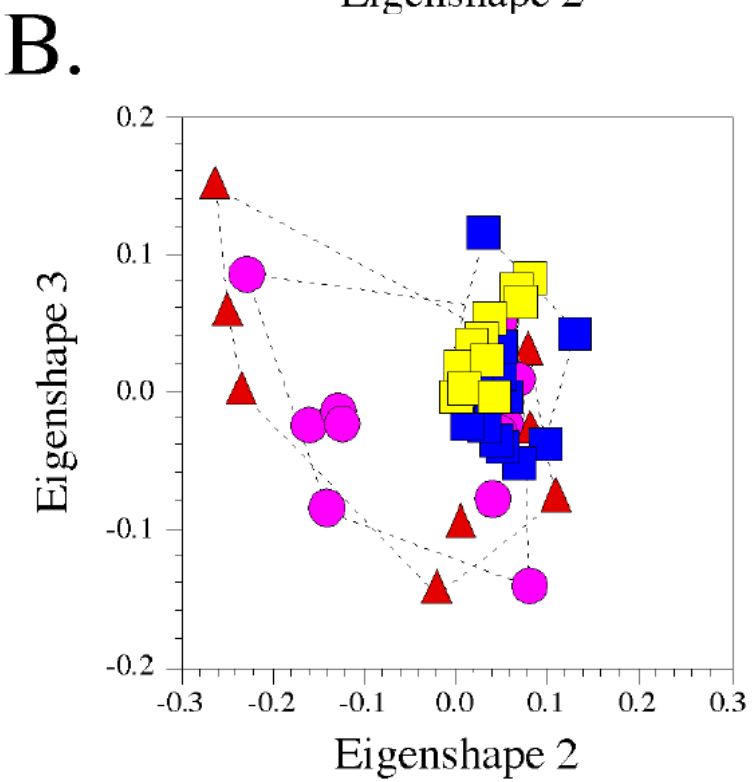

Figure 5. Results of MacLeod and Rose's (1993) shape analysis of modern mammalian distal phalanx (A) and proximal radial head (B) data. Symbols as follows: solid square = arboreal species, open squares = scansorial species, solid triangles = fossorial species, solid circles = cursorial species (see MacLeod and Rose 1993 Appendix 1 for species lists). Note that the ordination of species on the two most important distal phalanx shape-dissimilarity axes (eigenshape axes 2 and 3) separate the data set into three locomotor groups (with a small number of intergroup outliers) whereas the group separation in the proximal radial head analysis is much less pronounced. Since each locomotor group contains species from different mammalian clades, a functional signal may be overwhelmed by the phylogenetic signal in the latter analysis

Obrysová analýza: Fourierova analýza – Fourier analysis

Fourierova analýza s použitím rovnakých uhlov (equally spaced radii)

$$\theta = a_0 + \sum_{i=1}^{k} \left(a_i \cos(i\,\theta) + b_i \sin(i\,\theta) \right)$$

uhol θ varíruje od 0 do 2π, a_i b_i – Fourierove koeficienty *i*tej harmonickej funkcie, *k* – maximálny počet harmon. funkcií: *k*<*p*/2

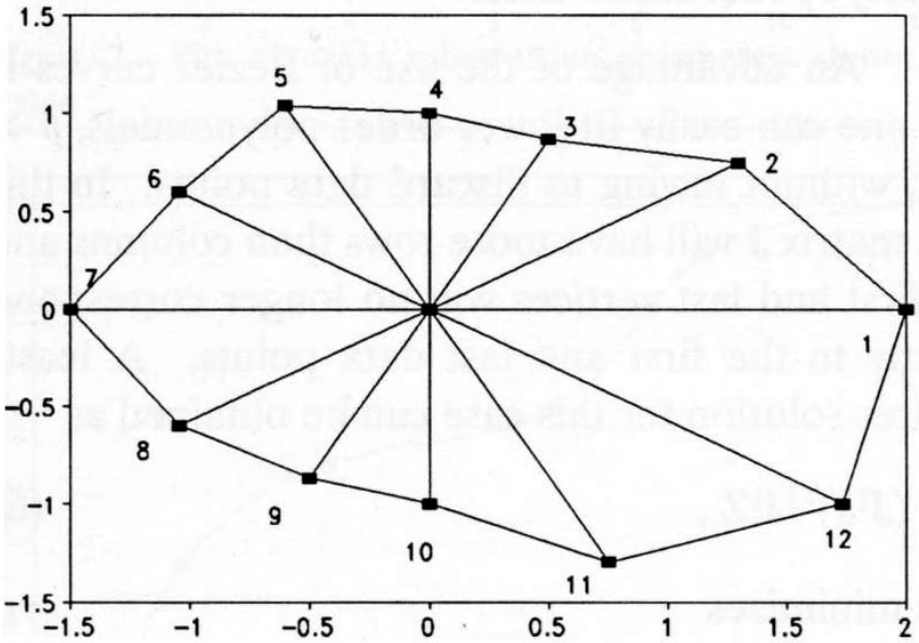

$$a_i = \sqrt{\frac{2}{p}} \sum_{j=1}^{p} \theta_j \cos(i\,\theta_j)$$

$$b_i = \sqrt{\frac{2}{p}} \sum_{j=1}^{p} \theta_j \sin(i\,\theta_j)$$

$$a_0 = \sqrt{\frac{1}{p}} \sum_{j=1}^{p} \theta_j$$

$$b_0 = 0 \ .$$

Rohlf (1990, „Blue Book“)

Fourierova analýza – Fourier analysis

Fourierova analýza s použitím rovnakých uhlov (equally spaced radii)

Table 7: Lengths, ρ, of radii at an angle θ and Fourier coefficients for harmonics 0 through 6.

θ	ρ	i	a_i	b_i
0.00000	2.0	0	1.34167	0.00000
0.52360	1.5	1	0.65427	-0.20813
1.04720	1.0	2	0.85732	-0.42426
1.57080	1.0	3	0.08165	-0.20412
2.09440	1.2	4	0.08165	0.07071
2.61799	1.2	5	-0.12355	0.00400
3.14159	1.5	6	0.12247	0.00000
3.66519	1.2			
4.18879	1.0			
4.71239	1.0			
5.23599	1.5			
5.75959	2.0			
6.28319	2.0			

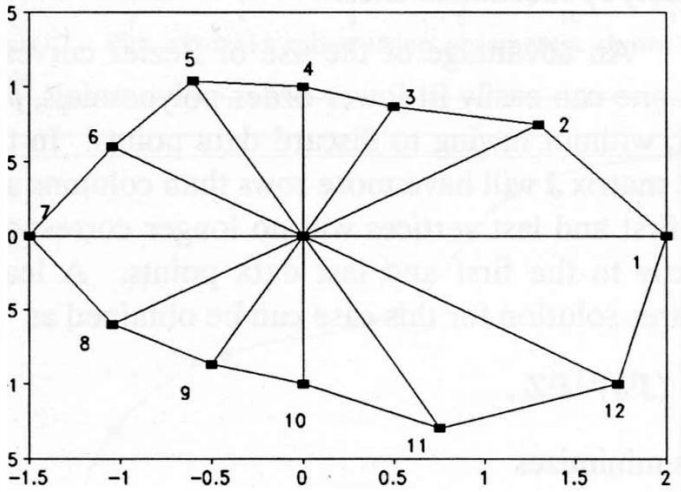

Rohlf (1990, „Blue Book“)

Fourierova analýza – Fourier analysis

Fourierova analýza tangentných uhlov (tangent angles)

$$\varphi^*(t) = \varphi(t) - t$$

Table 8. Zahn and Roskies (1972) ϕ^* values and their Fourier coefficients for the example data of Table 7.

t	ϕ	ϕ^*	i	a_i	b_i
0	2.32241	0	0	-0.34626	
0.71074	2.99739	-0.03575	1	0.17595	-0.10944
1.26974	2.87979	-0.71236	2	0.91564	0.26300
1.62813	3.07630	-0.87424	3	-0.15540	0.02055
2.04442	-2.35619	-0.43984	4	-0.02769	0.37984
2.47448	-2.22569	-0.73939			
2.99824	-0.91591	0.04663			
3.52200	-0.45831	-0.01954			
3.93829	-0.26180	-0.23932			
4.29668	-0.37940	-0.71530			
4.85568	0.29558	-0.59933			
5.56642	1.30900	-0.29665			

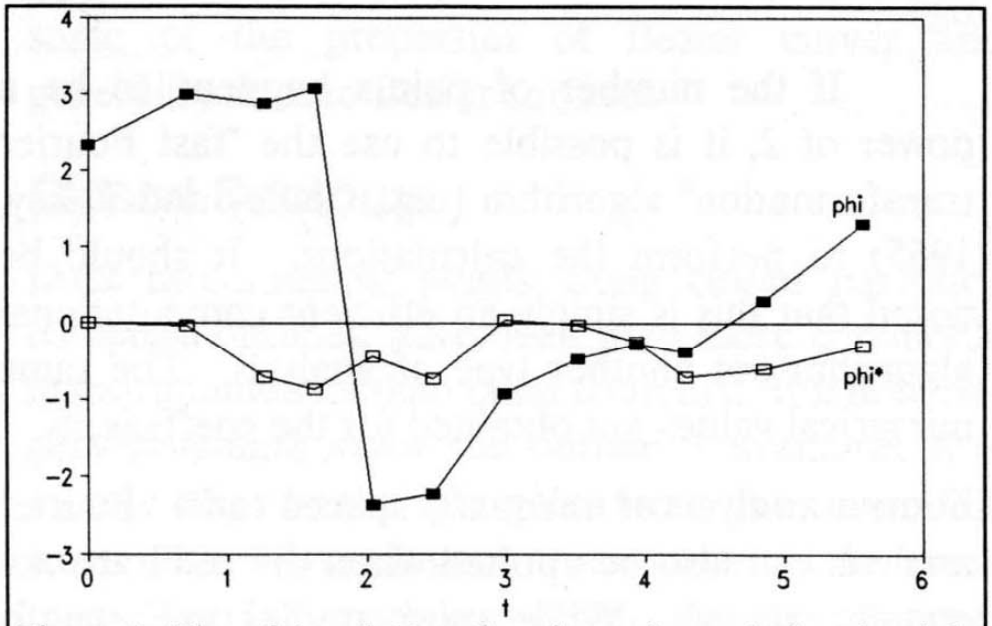

Figure 6. Plot of ϕ and ϕ^* as functions of cumulative chordal distance t.

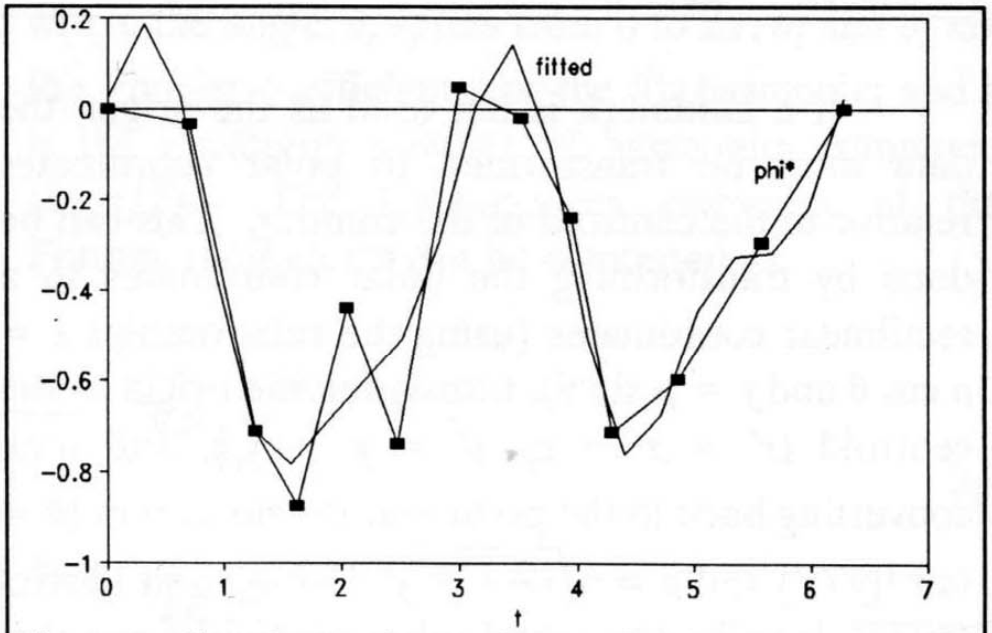

Figure 7. Plot of ϕ^* and an estimate of ϕ^* based on the first four harmonics.

Rohlf (1990, „Blue Book“)

Fourierova analýza – Fourier analysis

Eliptická Fourierova analýza (elliptic Fourier analysis)

Pozície bodov a krokov na obryse sú charakterizované x a y súradnicami.

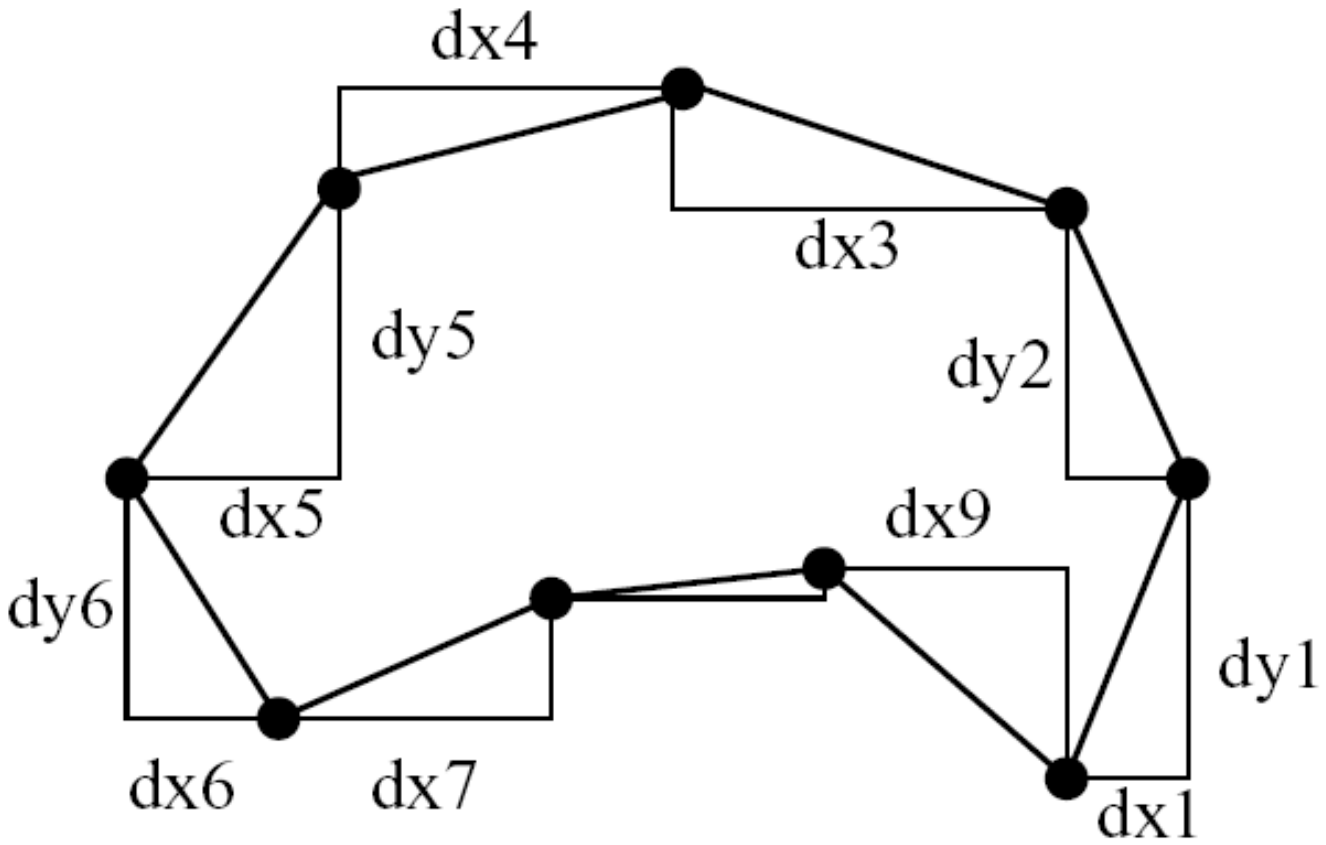

Fourierova analýza – Fourier analysis

Eliptická Fourierova analýza (elliptic Fourier analysis)

Funkcia, ktorú hľadáme, opisuje simultánnu zmenu súradníc, t.j. Δx a Δy v súlade so súborom harmonických funkcií. Pre každú harmonickú funkciu sa odvodzujú 4 koeficienty (dva pre horizontálne súradnice a dva pre vertikálne súradnice), okrem toho sa počítajú dve konštanty.

Fourierove koeficienty pre *k*tu harmonickú funkciu a *x* projekciu obrysu sa počítajú nasledovne:

$$A_k = \frac{T}{2p^2\pi^2} \sum_{i=1}^{p} \frac{\Delta x_i}{\Delta t_i} \left(\cos \frac{2\pi k t_i}{T} - \cos \frac{2\pi k t_{i-1}}{T} \right)$$

$$B_k = \frac{T}{2p^2\pi^2} \sum_{i=1}^{p} \frac{\Delta x_i}{\Delta t_i} \left(\sin \frac{2\pi k t_i}{T} - \sin \frac{2\pi k t_{i-1}}{T} \right)$$

$\Delta x_i = x_i - x_{i-1}$ – tetivová vzdialenosť kroku medzi bodmi *i* a *i-1*

t_i – kumulatívna dĺžka krokov po krok *i*

T – celková dĺžka obrysu

Rohlf (1990, „Blue Book“)

Konštanta pre súradnice x sa počíta nasledovne:

$$A_0 = x_0 +$$

$$\frac{1}{T}\sum_{i=1}^{p}\left[\frac{\Delta x_i}{2\Delta t_i}\left(t_i^2 - t_{i-1}^2\right) + \left[\sum_{j=1}^{i-1}\Delta x_j - \frac{\Delta x_i}{\Delta t_i}t_{i-1}\right]\Delta t_i\right]$$

Fourierove koeficienty pre *k*tu harmonickú funkciu a *y* projekciu obrysu sa počítajú ekvivalentne.

Pre celú krivku, *n* harmonických funkcií a *t* z intervalu 0 - 2π potom platí:

$$x(t) = A_0 + \sum_{k=1}^{n} A_k \cos kt_k + B_k \sin kt_{k-1}$$

$$y(t) = C_0 + \sum_{k=1}^{n} C_k \cos kt_k + D_k \sin kt_{k-1}$$

Fourierove koeficienty sa môžu potom použiť do ďalších analýz – PCA, zhlukovacia analýza, diskriminačná analýza ...

Fourierova analýza – Fourier analysis

Eliptická Fourierova analýza (elliptic Fourier analysis)

θ	ρ
0.00000	2.0
0.52360	1.5
1.04720	1.0
1.57080	1.0
2.09440	1.2
2.61799	1.2
3.14159	1.5
3.66519	1.2
4.18879	1.0
4.71239	1.0
5.23599	1.5
5.75959	2.0
6.28319	2.0

Table 9. Elliptic Fourier coefficients for the example data of Table 7.

i	A_i	B_i	C_i	D_i
0	0.31460	—	-0.09995	—
1	1.56468	-0.27246	0.00959	1.13297
2	-0.01796	0.00444	0.00135	0.03388
3	0.06718	-0.03061	0.08219	0.03999

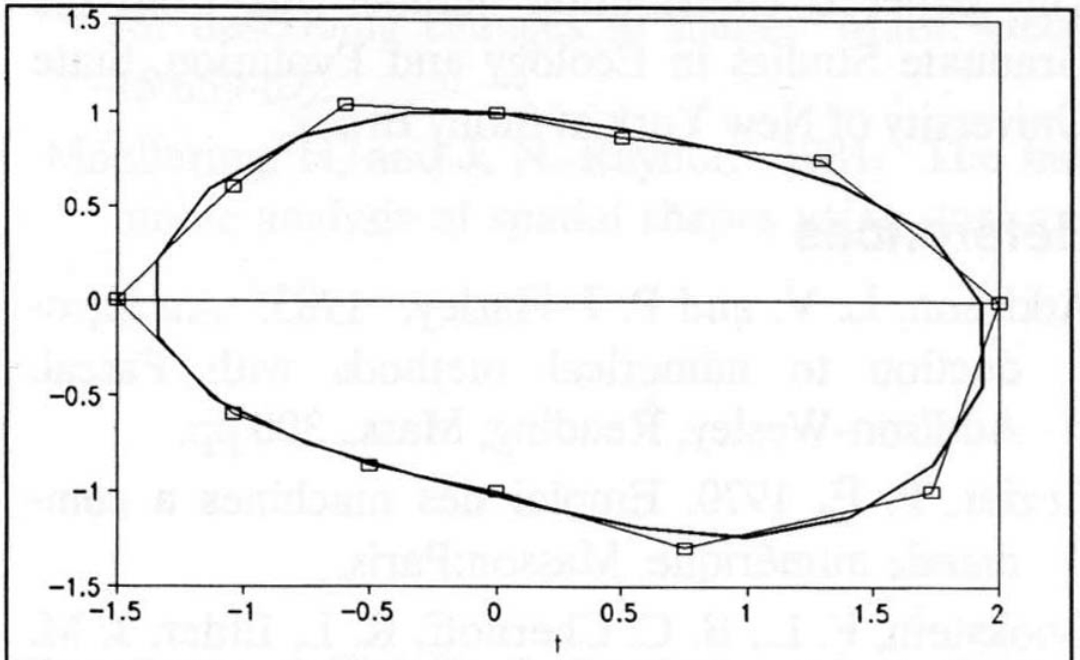

Figure 8. Plot of elliptic Fourier function based on the first 3 harmonics for the example data (squares connected with thin lines) of Table 7.

Rohlf (1990, „Blue Book“)

Paleobiology, 24(3), 1998, pp. 359–370

Ontogeny of *Trimerocephalus lelievrei* (Trilobita, Phacopida), a representative of the Late Devonian phacopine paedomorphocline: a morphometric approach

Catherine Crônier, Sabrina Renaud, Raimund Feist, and Jean-Christophe Auffray

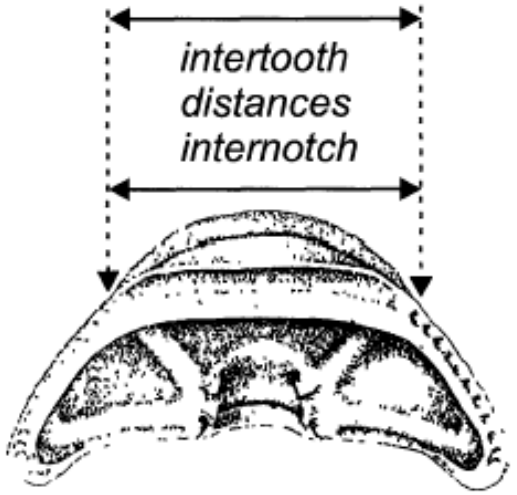

64 bodov charakterizujúcich obrys

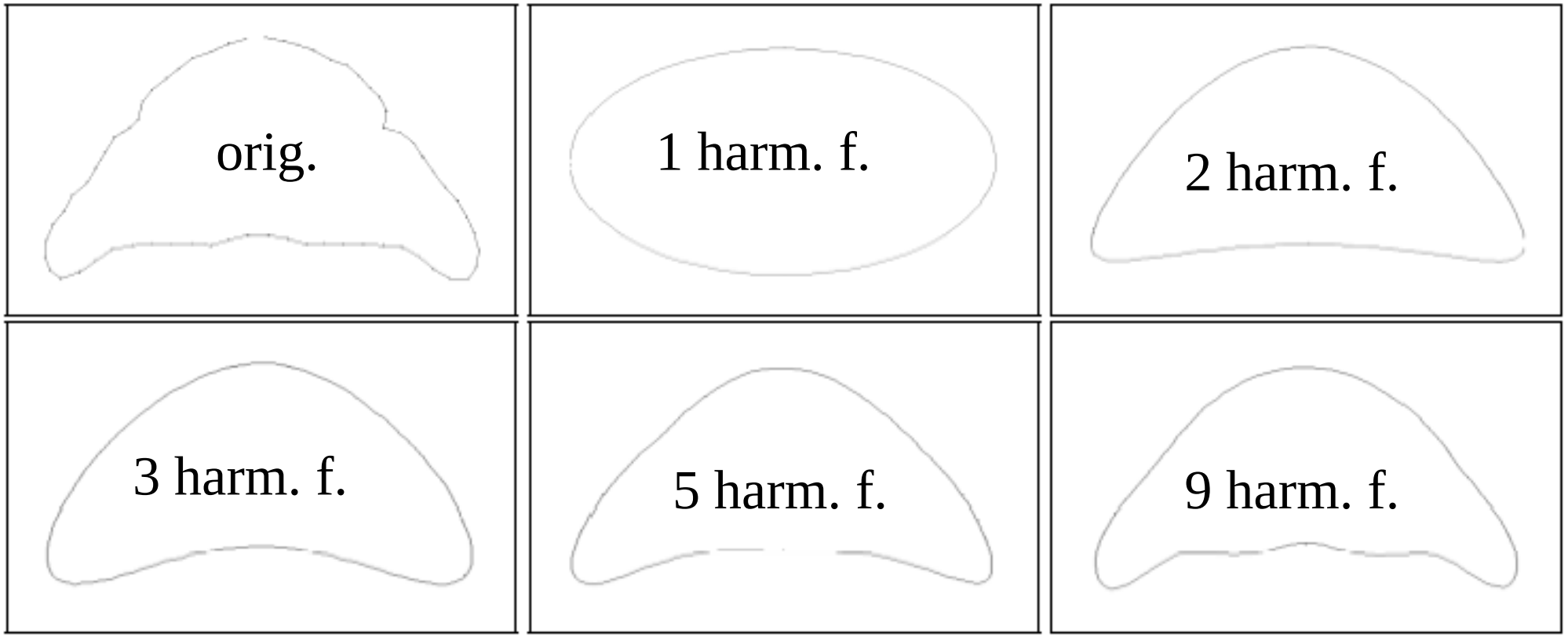

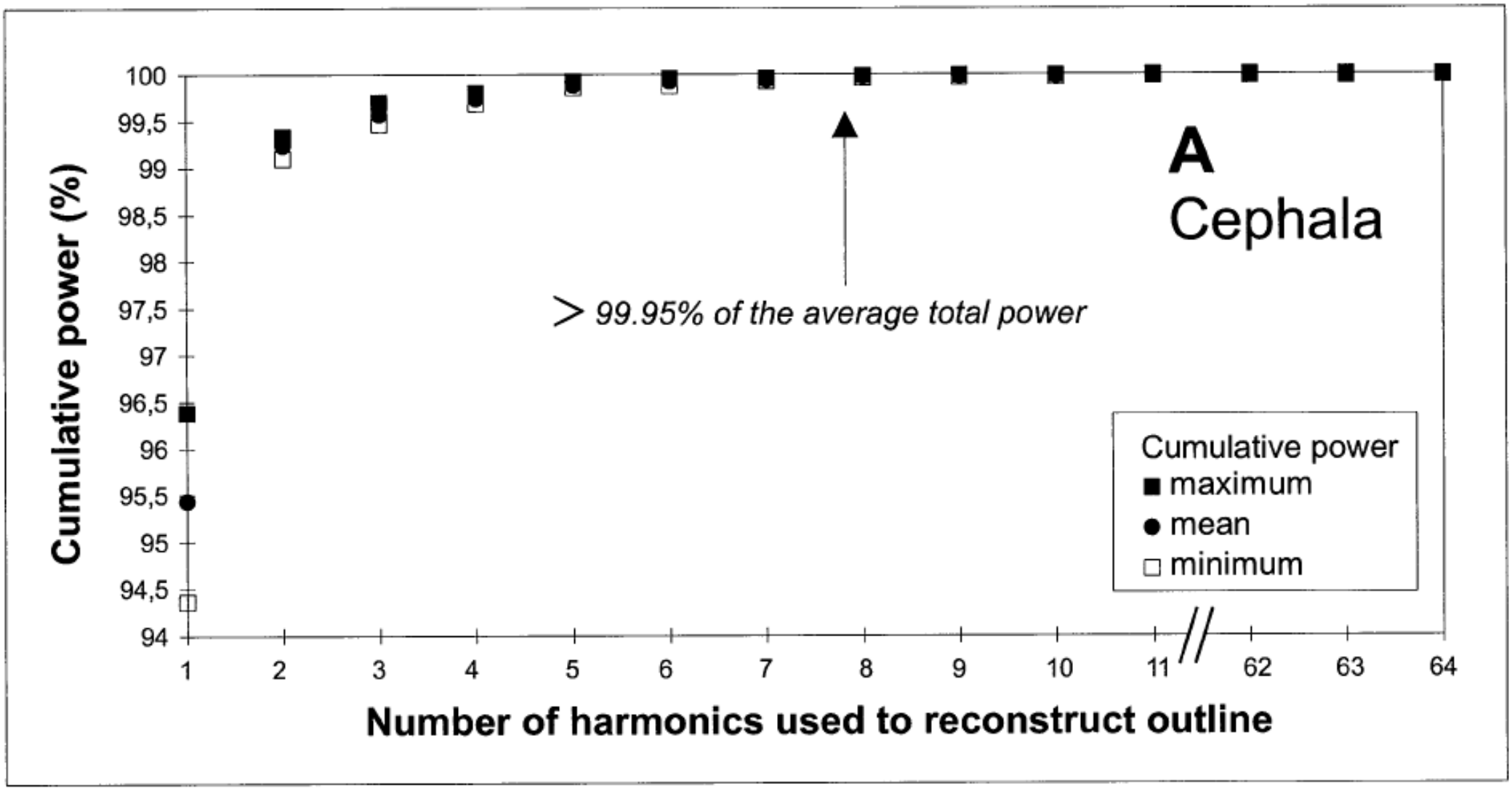

FIGURE 2. Average Fourier power (or variance) spectrum for cephala (A) and pygidia (B). The Fourier power for the n^{th} harmonic is $(an^2 + bn^2 + cn^2 + dn^2)/2$. For any outline, the total power is calculated as the sum, from 1 to 64, of individual harmonic powers where 64 is equal to the Nyquist frequency. For both cephala and pygidia, 99.95% of the power is described by the first eight harmonics, represented by arrows.

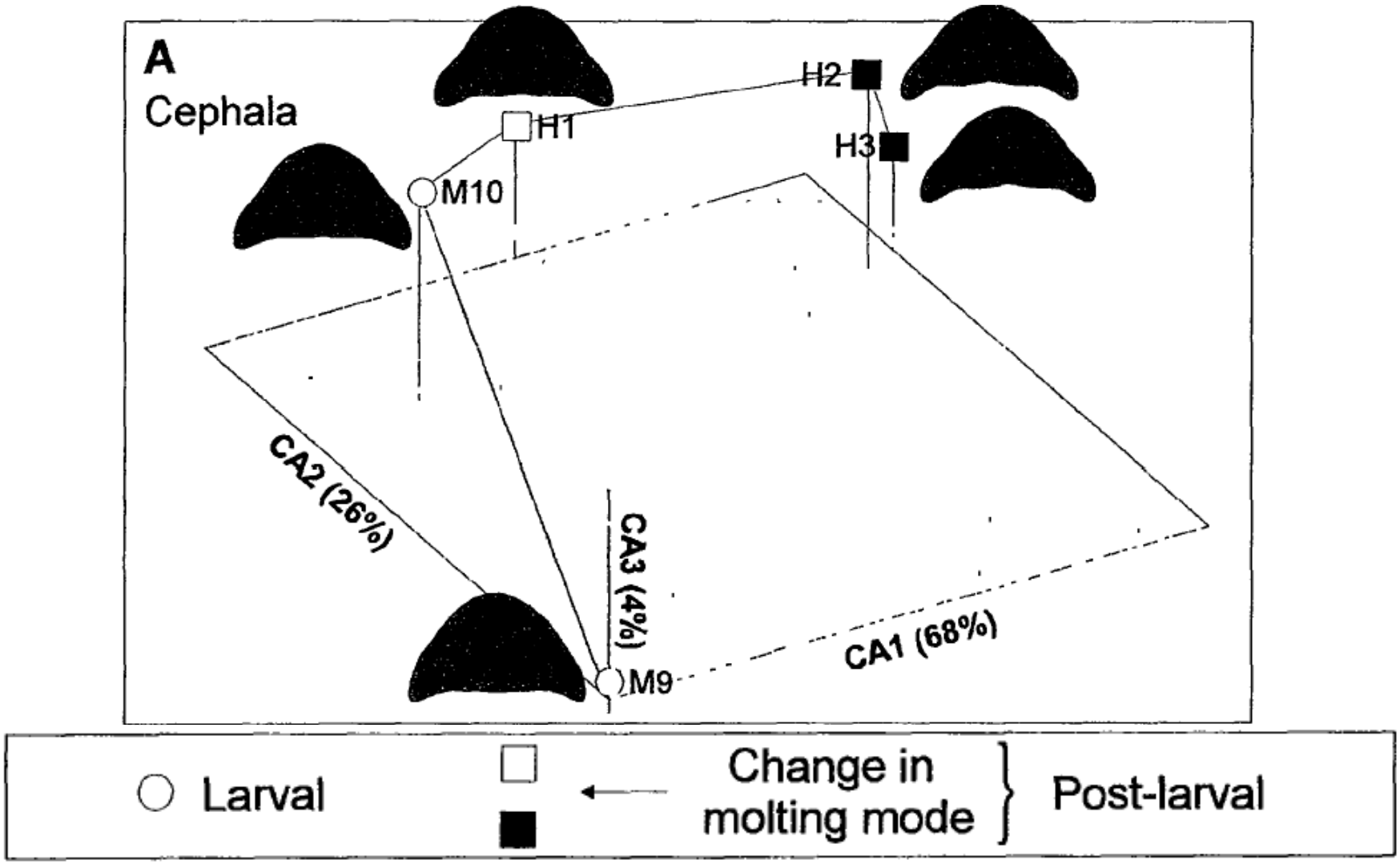

FIGURE 5. Location of the instar means and their reconstructed outlines in the canonical space corresponding to standardized Fourier coefficients. Axes CA1–3 represent 68%, 26%, and 4%, respectively, of the among-instar variance for cephala

Paleobiology, 22(2), 1996, pp. 255–265

Fourier analysis applied to *Stephanomys* (Rodentia, Muridae) molars: nonprogressive evolutionary pattern in a gradual lineage

Sabrina Renaud, Jacques Michaux, Jean-Jacques Jaeger, and Jean-Christophe Auffray

In order to determine the rank of the last harmonic that has to be retained for a satisfactory description of the outline, we have considered the accuracy of the information provided by these harmonics. For that purpose, six repeated measurements were performed on a sample of eight upper molars. The coefficient of variation of the harmonics amplitude $a_n^2 + b_n^2 + c_n^2 + d_n^2$ increases strongly for the eighth harmonic and the subsequent ones (Fig. 3A). From this harmonic onward, the noise, caused by variation of such factors as light and positioning of the tooth during optical measurement, reduced the reproducibility of the measurement. Hence, the coefficients from the eighth harmonic onward were excluded in the statistical analysis.

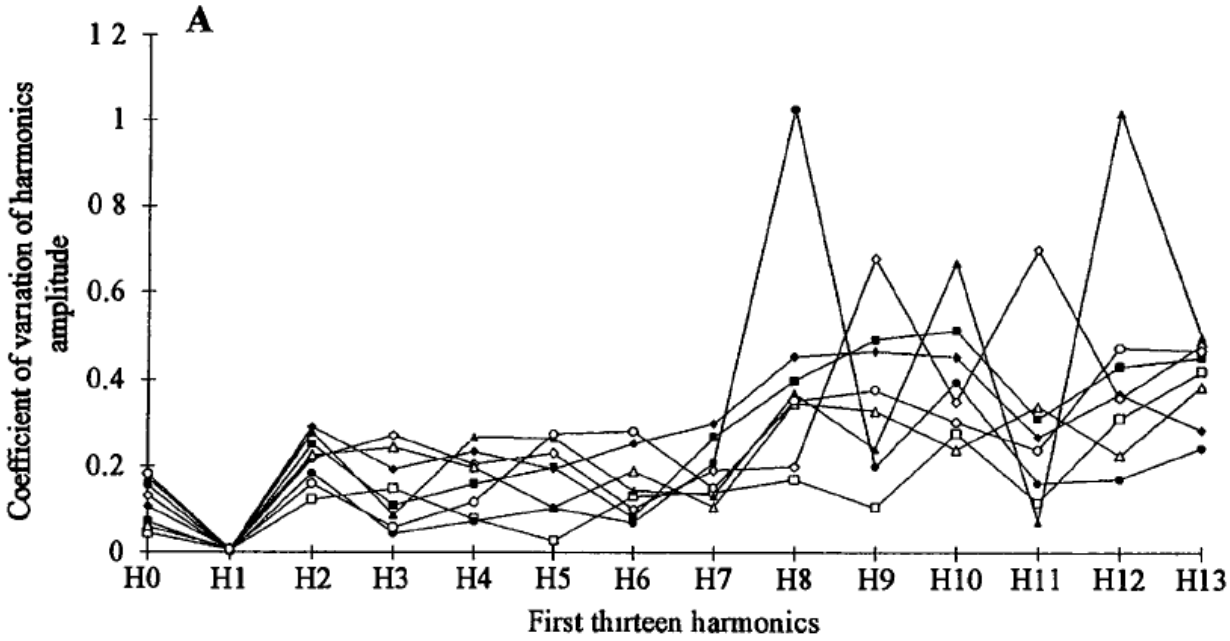

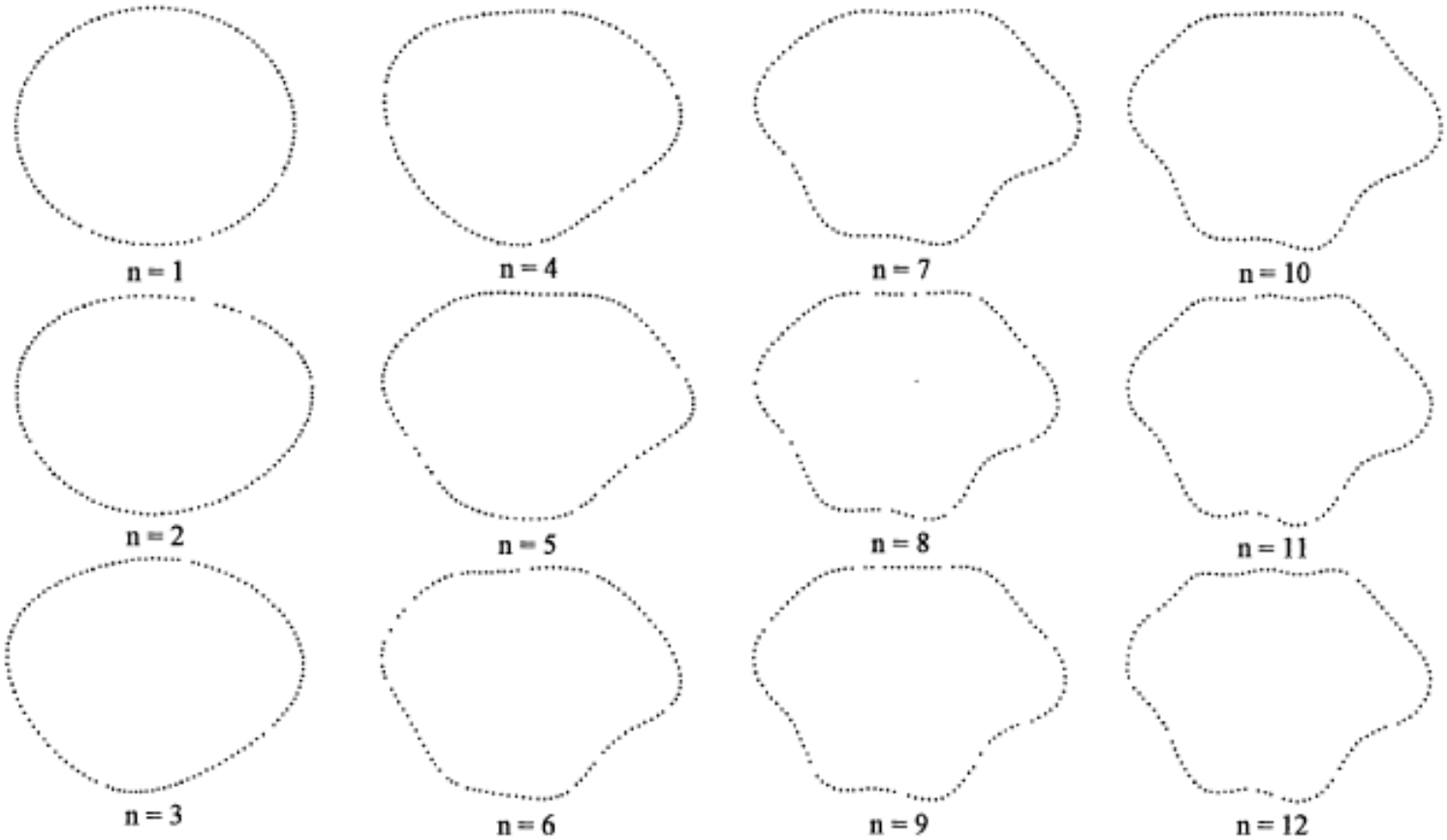

FIGURE 2. Reconstruction of a first upper molar for the successive cumulative contribution of the first twelve harmonics.

Paleobiology, 28(4), 2002, pp. 435–448

Ontogenetic and evolutionary patterns of shape differentiation during the initial diversification of Paleocene acarininids (planktonic foraminifera)

Frédéric Quillévéré, Vincent Debat, and Jean-Christophe Auffray

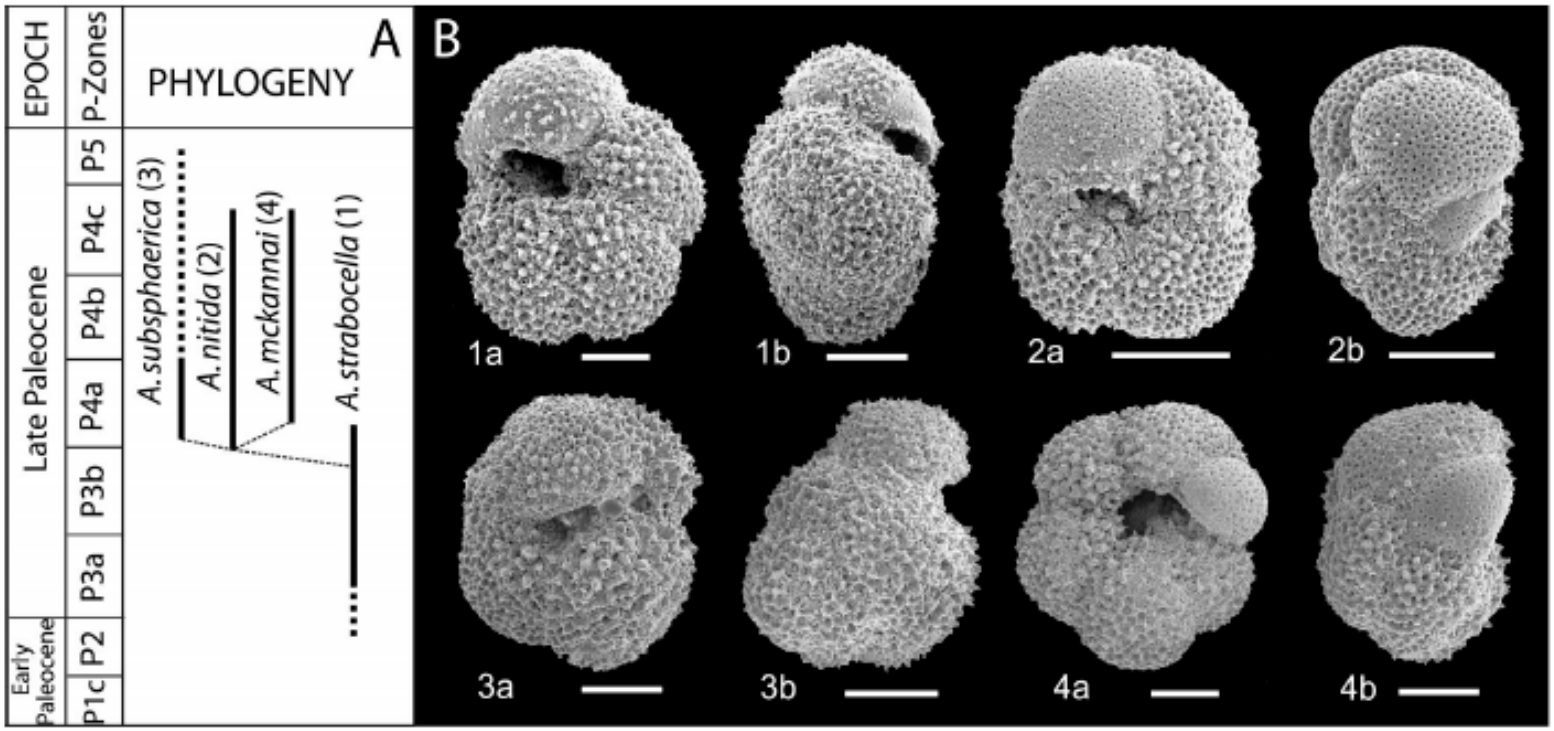

FIGURE 1. A, Phylogenetic reconstruction of Paleocene acarininids studied in this paper (dashed line represents range extension at southern high latitude sites). After Berggren and Norris (1997), Olsson et al. (1999), and Quillévéré et al. (2000). B, Scanning electron photomicrographs of representative Paleocene acarininids from ODP Hole 761B. 1: umbilical (a) and edge (b) views of *A. strabocella* from 761B–18X–2: 10–12 cm. 2: umbilical (a) and edge (b) views of *A. nitida* from 761B–18X–2: 10–12 cm. 3: umbilical (a) and edge (b) views of *A. subsphaerica* from respectively 761B–17X–4, 10–12 cm and 761B–17X–3: 10–12 cm. 4: umbilical (a) and edge (b) views of *A. mckannai* from 761B–17X–1: 10–12 cm. Scale bar, 100 μm.

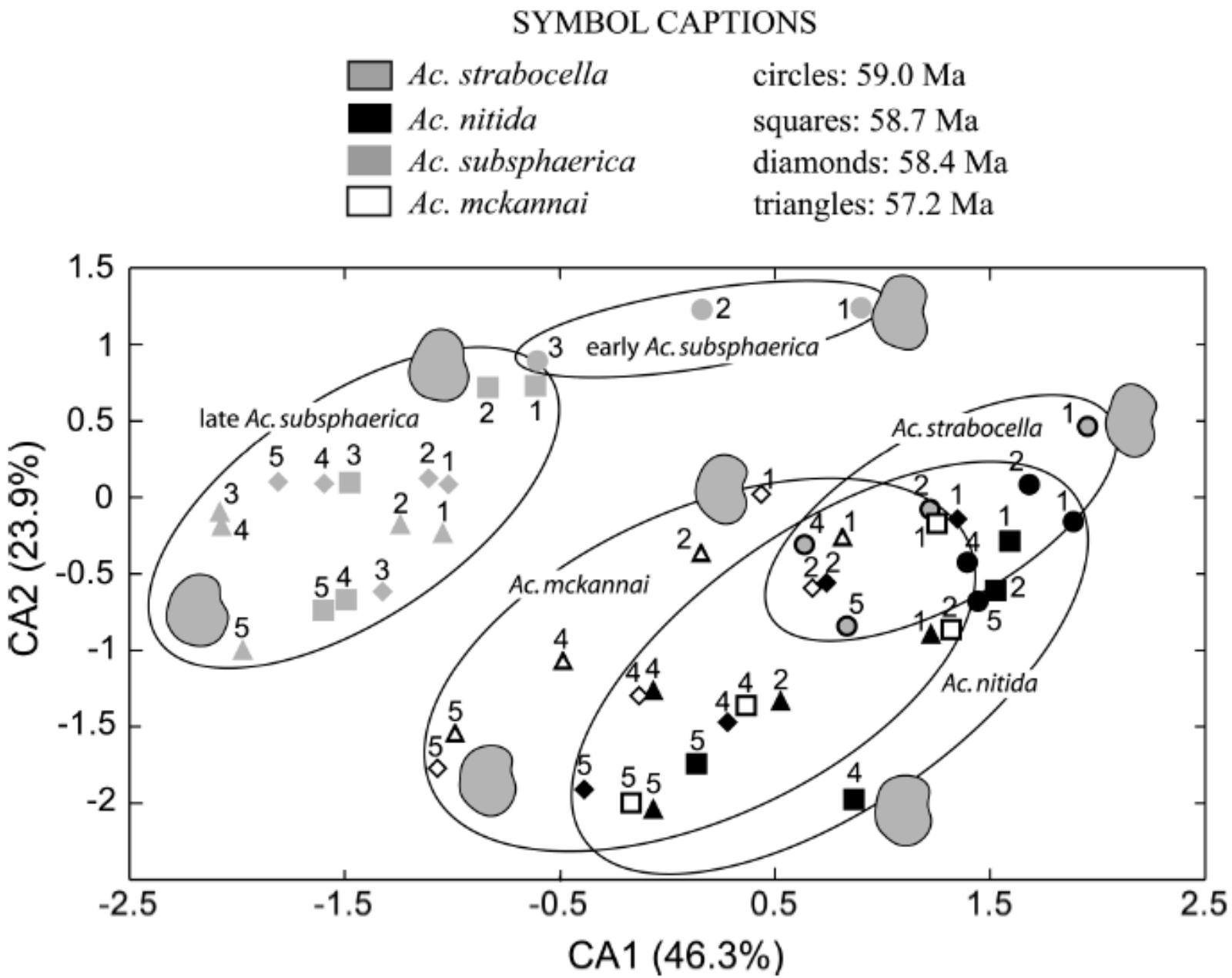

FIGURE 4. Location of the sample means in the canonical plane of the MANOVA performed on standardized Fourier coefficients of ontogenetic stages and stratigraphic horizons of the acarininid species considered in this study. The species name is expressed by the color of the symbols. The age of the samples analyzed is expressed by the shape of the symbols. Labels correspond to the different test size fractions (1 = 63–125 μm; 2 = 125–150 μm; 3 = 150–212 μm; 4 = 212–250 μm; and 5 > 250 μm). Reconstructed outlines for some group means visualize shape changes in the plane defined by the first two canonical axes. These reconstructed mean outlines of selected groups have been obtained using inverse Fourier Transform.

Euphytica **102:** 143–149, 1998.

Evaluation of variation of root shape of Japanese radish (*Raphanus sativus* L.) based on image analysis using elliptic Fourier descriptors

Hiroyoshi Iwata[1], Satoshi Niikura[2], Seiji Matsuura[2], Yasushi Takano[1] & Yasuo Ukai[1]

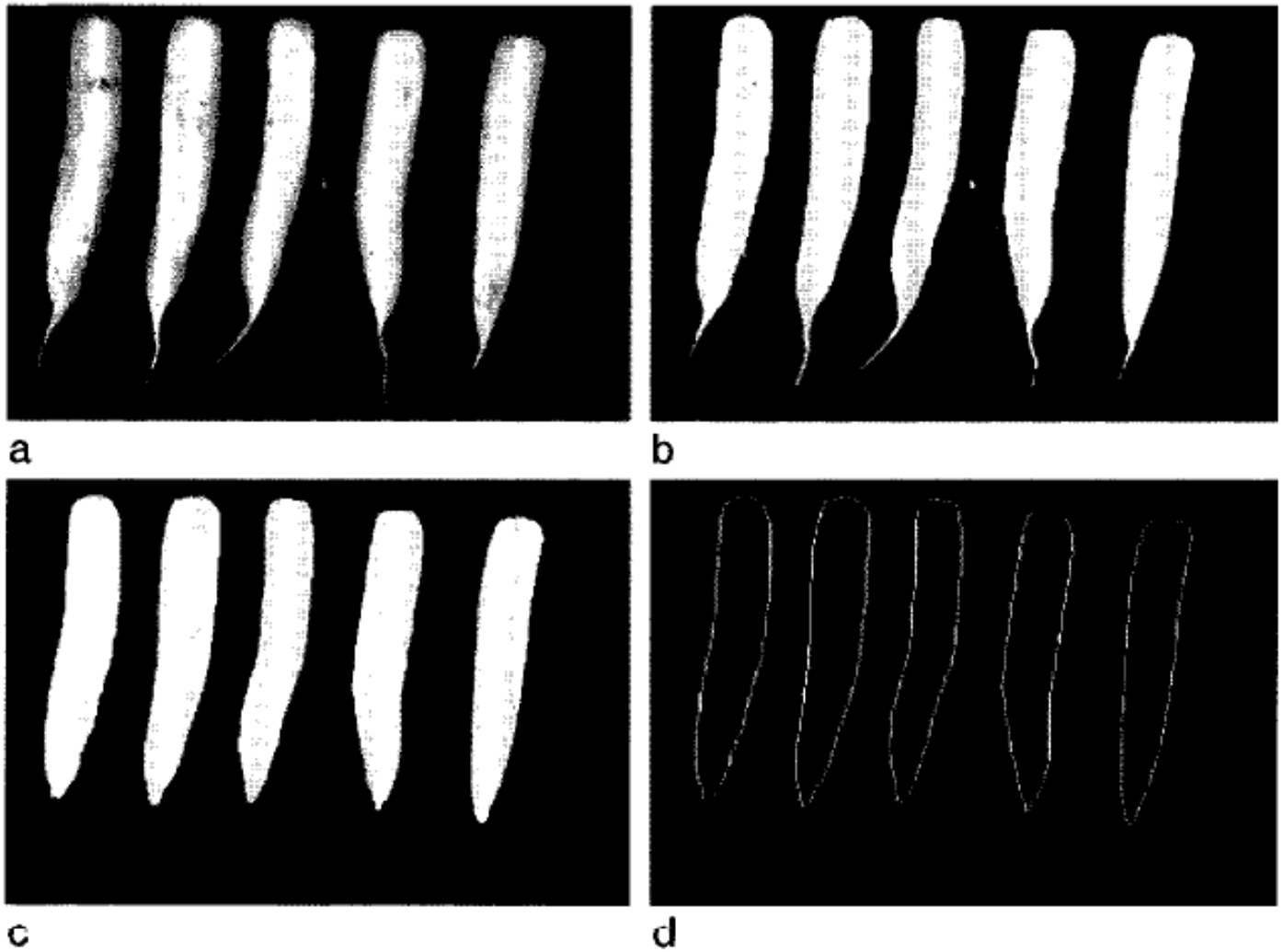

Figure 2. Series of image processing which extracts chain-coded contour from red digital image; a: red digital image of 256 gray levels; b: binary image; c: image after noise reduction, erosion, dilation, and filling holes; d: extracted contours.

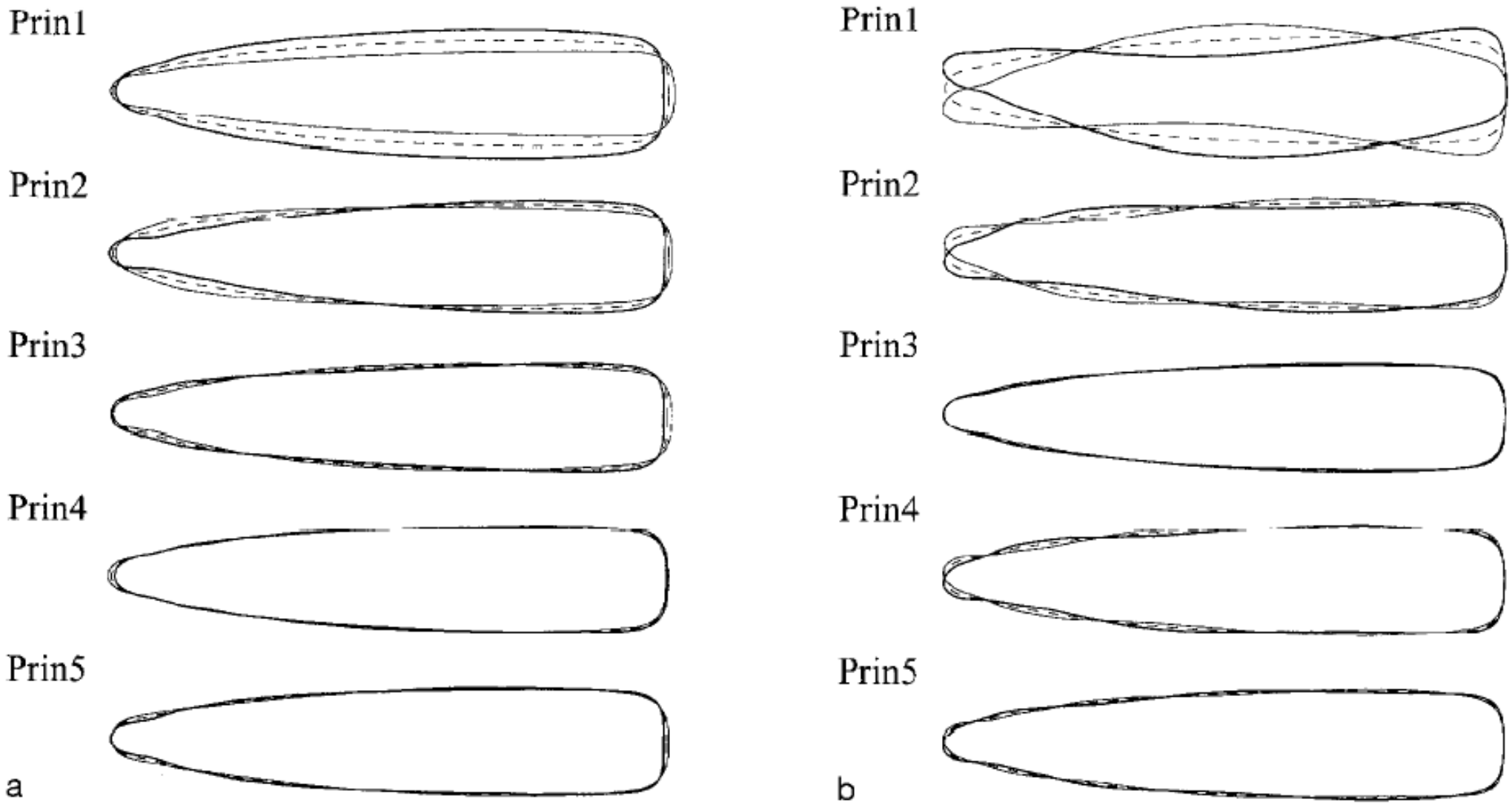

Figure 3. The shape variation which can be accounted for by each principal component. Each shape was reconstructed from the coefficients which were calculated by letting the score on the corresponding principal component be equal to mean with plus or minus two times standard deviation and the scores on the remaining component zero. (a) symmetrical variation from group A coefficients. (b) asymmetrical variation from group B coefficients. Dashed line, thick solid line, and thin solid line stand for mean, mean + 2S.D., mean - 2S.D.

Botanical Journal of the Linnean Society (2000), *132:* 79–95. With 10 figures

doi: 10.1006/bojl.1999.0292, available online at http://www.idealibrary.com on IDEAL®

Geographic variation and plasticity of leaf shape and size in *Begonia dregei* and *B. homonyma* (Begoniaceae)

TRACY McLELLAN FLS*

Department of Molecular and Cell Biology, University of the Witwatersrand, Private Bag 3, Wits 2050, South Africa

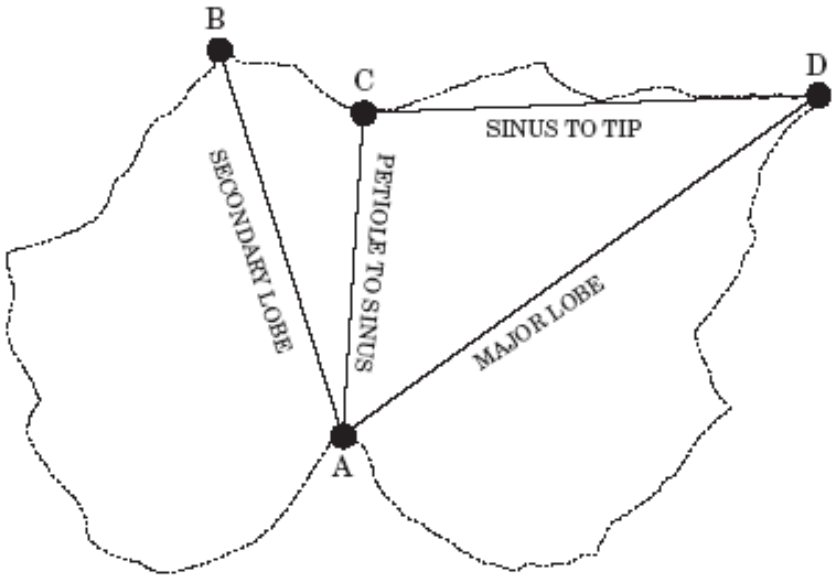

Figure 2. Measurement taken on digitized leaf outlines. Point A was the first point in the outline at the junction of the petiole and the lamina; points B and C were designated during digitizing, and point D was found by finding the point on the outline at the greatest distance from point A. Part perimeter is the distance along the perimeter between points C and D.

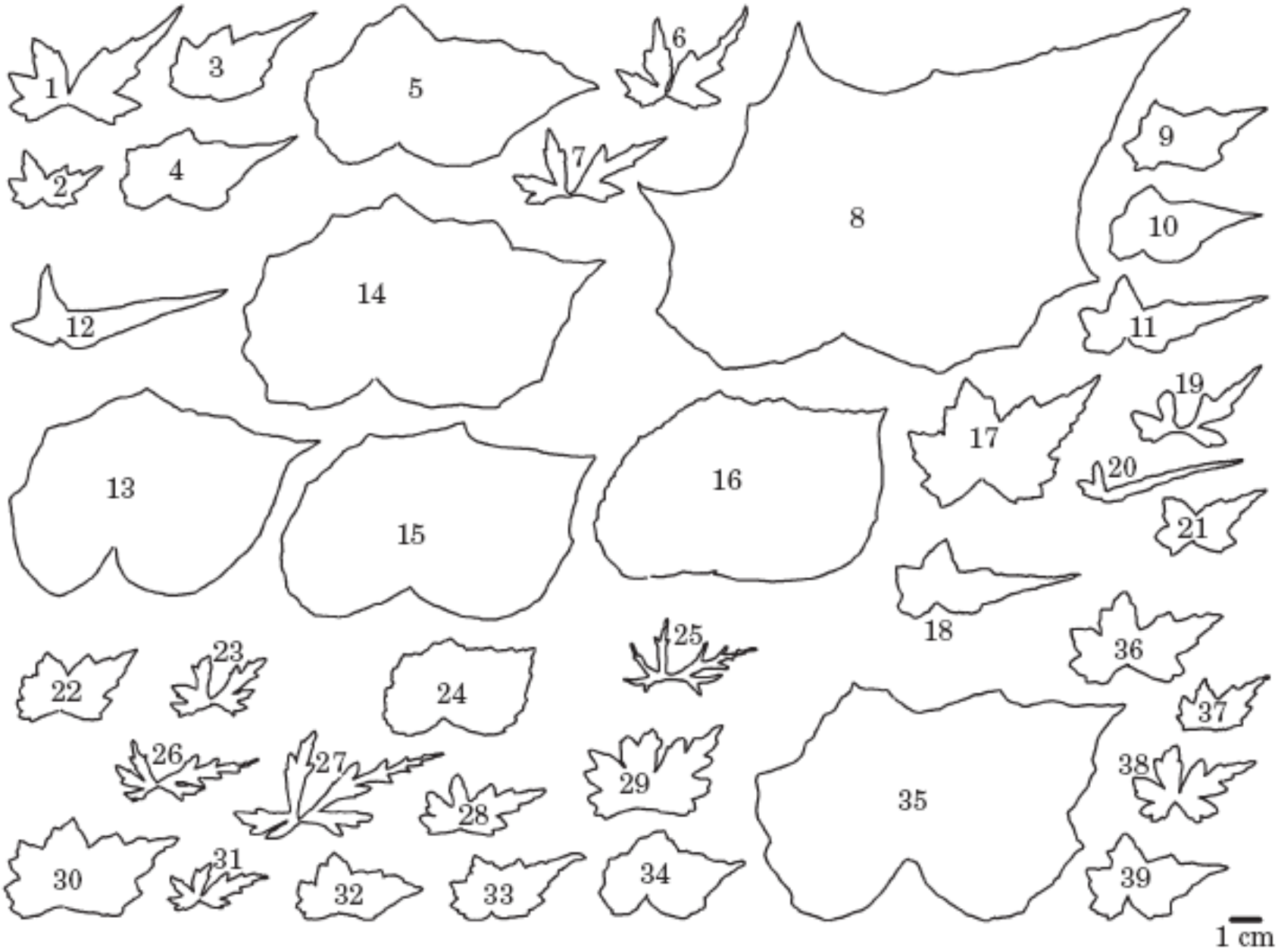

Figure 3. Silhouettes of representative leaves from each of 39 populations. Population numbers are as in Table 1.

The first six harmonics of elliptic Fourier coefficients (EFC) were calculated, normalized, and the power series was calculated from the *x,y* coordinates of the images (McLellan & Endler, 1998). These coefficients were then averaged over all the leaves taken from each plant, and the means of the coefficients were used in the principal component analysis.

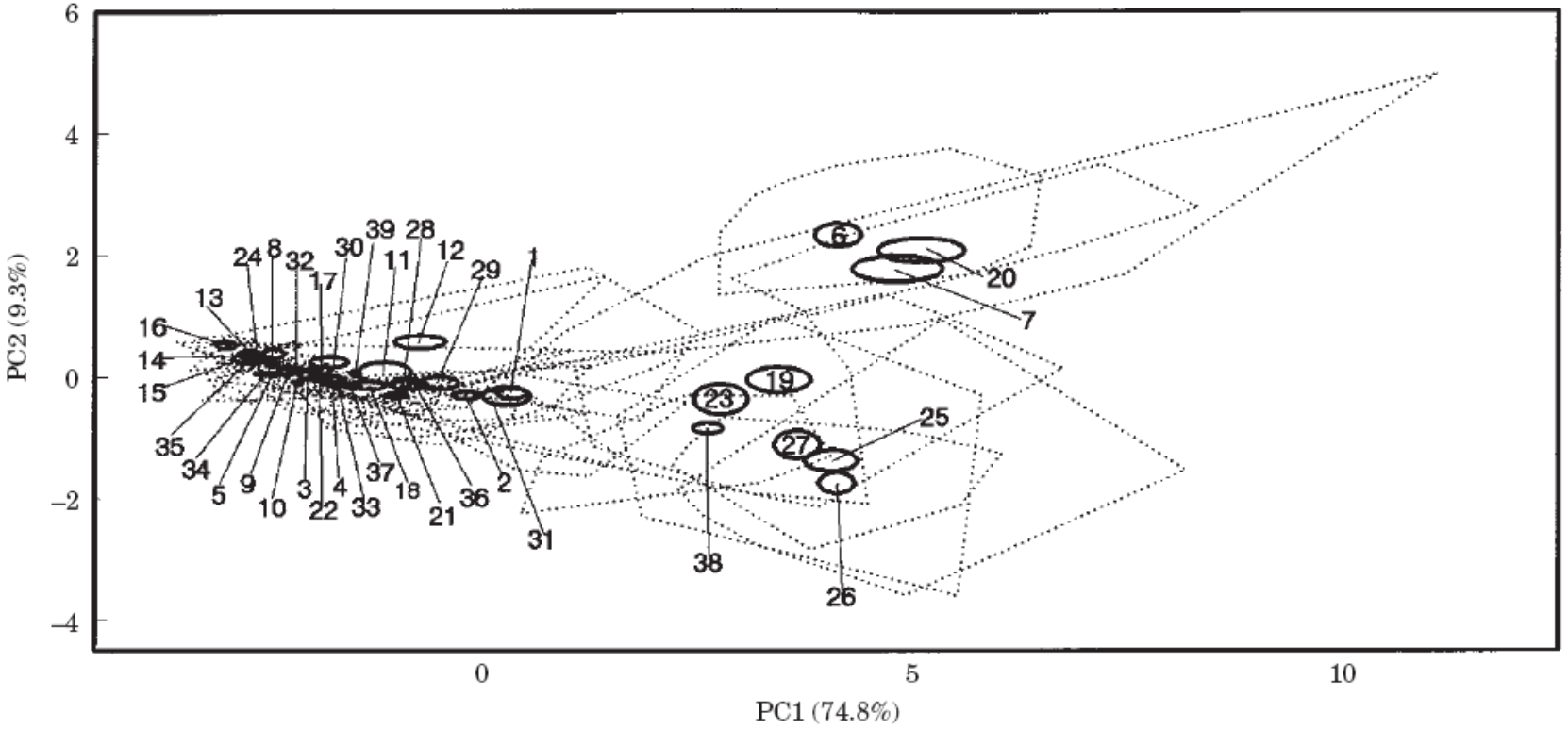

Figure 6. Plot of the first two principal components of the first five harmonics of elliptic Fourier coefficients for 39 population samples.

Ellipses are one standard error from the means of the PCs for each population, and polygons are defined by samples with extreme values for each population.